AD-A166 112 ANALYSIS AND PREDICTION OF OUTRUNNING GROUND MOTION(U) 1/1
APPLIED RESEARCH ASSOCIATES INC ALBUQUERQUE NM
S HASSIOTIS 23 JAN 85 DNA-TR-85-155 DNA001-84-C-0125
UNCLASSIFIED F/G 10/3 NL

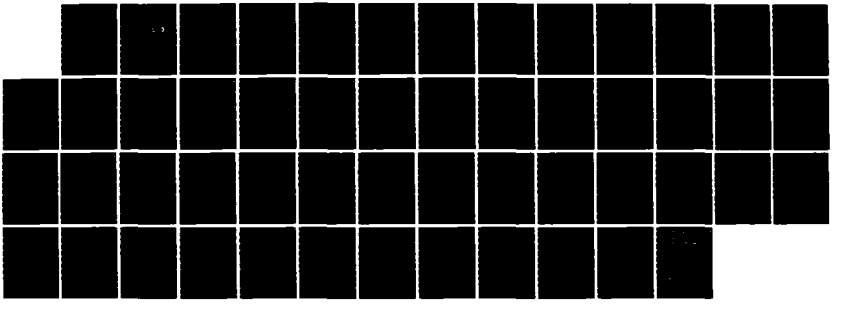

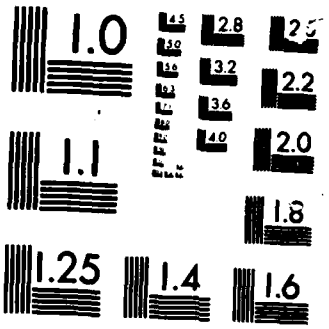

MICROCOPY RESOLUTION TEST CHART

DNA-TR-85-155

ANALYSIS AND PREDICTION OF OUTRUNNING GROUND MOTION

Sophia Hassiotis
Applied Research Associates, Inc.
4300 San Mateo Blvd. NE, Suite A220
Albuquerque, NM 87110

23 January 1985

Technical Report

CONTRACT No. DNA 001-84-C-0125

THIS WORK WAS SPONSORED BY THE DEFENSE NUCLEAR AGENCY
UNDER RDT&E RMSS CODE B344084466 Y99QMXSB00008 H2590D.

Prepared for
Director
DEFENSE NUCLEAR AGENCY
Washington, DC 20305-1000

Destroy this report when it is no longer needed. Do not return to sender.

PLEASE NOTIFY THE DEFENSE NUCLEAR AGENCY, ATTN: STTI, WASHINGTON, DC 20305-1000, IF YOUR ADDRESS IS INCORRECT, IF YOU WISH IT DELETED FROM THE DISTRIBUTION LIST, OR IF THE ADDRESSEE IS NO LONGER EMPLOYED BY YOUR ORGANIZATION.

UNCLASSIFIED

SECURITY CLASSIFICATION OF THIS PAGE

AD-A166 112

REPORT DOCUMENTATION PAGE

Form Approved
OMB No 0704-0188
Exp. Date: Jun 30, 1986

1a REPORT SECURITY CLASSIFICATION UNCLASSIFIED	1b RESTRICTIVE MARKINGS
2a SECURITY CLASSIFICATION AUTHORITY N/A since Unclassified	3 DISTRIBUTION / AVAILABILITY OF REPORT Approved for public release; distribution is unlimited.
2b DECLASSIFICATION / DOWNGRADING SCHEDULE N/A since Unclassified	
4 PERFORMING ORGANIZATION REPORT NUMBER(S)	5 MONITORING ORGANIZATION REPORT NUMBER(S) DNA-TR-85-155
6a NAME OF PERFORMING ORGANIZATION Applied Research Associates, Inc. 6b OFFICE SYMBOL (If applicable)	7a NAME OF MONITORING ORGANIZATION Director Defense Nuclear Agency
6c ADDRESS (City, State, and ZIP Code) 4300 San Mateo Blvd. NE, Suite A220 Albuquerque, NM 87110	7b ADDRESS (City, State, and ZIP Code) Washington, DC 20305-1000
8a NAME OF FUNDING / SPONSORING ORGANIZATION 8b OFFICE SYMBOL (If applicable)	9 PROCUREMENT INSTRUMENT IDENTIFICATION NUMBER DNA 001-84-C-0125
8c ADDRESS (City, State, and ZIP Code)	10 SOURCE OF FUNDING NUMBERS

PROGRAM ELEMENT NO	PROJECT NO	TASK NO	WORK UNIT ACCESSION NO
62715H	Y99QMXS	B	DH008148

11 TITLE (Include Security Classification)
ANALYSIS AND PREDICTION OF OUTRUNNING GROUND MOTION

12 PERSONAL AUTHOR(S)
Hassiotis, Sophia

13a TYPE OF REPORT	13b TIME COVERED	14 DATE OF REPORT (Year, Month, Day)	15 PAGE COUNT
Technical Report	FROM 831208 TO 850123	850123	52

16 SUPPLEMENTARY NOTATION
This work was sponsored by the Defense Nuclear Agency under RDT&E RMSS Code B344084466 Y99QMXSB00008 H2590D.

17 COSATI CODES			18 SUBJECT TERMS (Continue on reverse if necessary and identify by block number)	
FIELD	GROUP	SUB GROUP		
8	11		Outrunning	Prediction Procedure
19	4		Oscillatory Ground Motion	Wave Propagation
			Direct-Induced	Ground Shock Data

19 ABSTRACT (Continue on reverse if necessary and identify by block number)

With the advent of the hard mobile launcher, the need for an accurate prediction procedure for the outrunning ground shock (i.e., the wave that arrives before the airblast) has increased. Most methods developed in the past for the prediction of the outrunning wave concentrate on a limited number of HE experiments. This report describes the development of a new method to predict the outrunning portion of the ground shock. This method is an extension of the one developed by Sauer (1964). It is based on the empirical analysis of data provided by several recent HE experiments at various heights-of-burst. A characteristic velocity time history waveform, which is normalized by the outrunning velocity peak and a site dependent time scale factor, is introduced. The method is evaluated against data from several experiments and the results are considered satisfactory.

20 DISTRIBUTION / AVAILABILITY OF ABSTRACT	21 ABSTRACT SECURITY CLASSIFICATION
☐ UNCLASSIFIED/UNLIMITED ☒ SAME AS RPT ☐ DTIC USERS	UNCLASSIFIED

22a NAME OF RESPONSIBLE INDIVIDUAL	22b TELEPHONE (Include Area Code)	22c OFFICE SYMBOL
Betty L. Fox	(202) 325-7042	DNA/STTI

DD FORM 1473, 84 MAR 83 APR edition may be used until exhausted
All other editions are obsolete

SECURITY CLASSIFICATION OF THIS PAGE
UNCLASSIFIED

PREFACE

This report summarizes the work performed by Applied Research Associates on Task 3 of Contract DNA 001-84-C-0125. This task involved the analysis and modification of the prediction procedures for outrunning ground shock.

CONVERSION TABLE

PERTINENT CONVERSION FACTORS--
SI to U.S. CUSTOMARY UNITS OF MEASUREMENT

Parameter	To Convert From	To	Multiply By
Length	Meters (m)	Feet (ft)	3.28
Velocity	Meter/Second (m/s)	Feet/Second (ft/s)	3.28
Density	Kilograms/Cubic Meter (kg/m^3)	Pounds/Cubic Feet (pcf)	62.4×10^{-3}
Pressure or Stress	Mega Pascals (MPa)	Pounds/Square Inch (psi)	145
Impulse	Mega Pascals Seconds (MPa-s)	Pounds/Square Inch-s (psi-s)	145

TABLE OF CONTENTS

Section		Page
	PREFACE	1
	CONVERSION TABLE	2
	LIST OF ILLUSTRATIONS	4
	LIST OF TABLES	6
1	INTRODUCTION	7
2	PREVIOUS OUTRUNNING MODELS	10
3	DEVELOPMENT OF A CHARACTERISTIC WAVEFORM	17
	3.1. Test Site Geologies	17
	3.2. Time of Arrival	19
	3.3. Velocity Scaling Factor	23
	3.4. Time Scaling Factor	23
	3.5. Characteristic Wave	32
4	CONCLUSIONS AND RECOMMENDATIONS	42
	4.1. Conclusions	42
	4.2. Recommendations	42
	REFERENCES	43

LIST OF ILLUSTRATIONS

Figure		Page
1	Surface layer outrunning.	9
2	Outrunning due to layer refraction.	9
3	Outrunning waveform.	11
4	DIRECT COURSE and MIXED COMPANY data compared to the Sauer waveform.	12
5	Fits to normalized vertical velocities for various events.	15
6	Prediction of the ground shock arrival based on the site geology.	22
7	First peak of the outrunning wave vs. range-vertical.	24
8	First peak of the outrunning wave vs. range-horizontal.	25
9	DIRECT COURSE data vs. calculated outrunning ground motion (range = 305 m)	27
10	Calculated vertical and horizontal velocities with CAGGS--MIXED CO., range = 196 m, depth = 2.7 m, impedance ratio = 3.9	28
11	Calculated vertical and horizontal velocities with CAGGS--MIXED CO., range = 196 m, Depth = 5.8 m	29
12	Calculated vertical and horizontal velocities with CAGGS--MIXED CO., range = 196 m, depth = 2.7 m, impedance ratio = 2.88	30
13	Calculated vertical and horizontal velocities with CAGGS--MIXED CO., range = 196 m, depth = 2.7 m, impedance ratio = 5.78	31
14	Different data plotted with the new scaling factors.	33
15	Characteristic vertical velocity waveform.	34
16	Characteristic horizontal velocity waveform.	35

LIST OF ILLUSTRATIONS (Concluded)

Figure		Page
17	DIRECT COURSE data vs. calculated vertical and horizontal velocities. Range = 466 m	36
18	MILL RACE data vs. calculated outrunning vertical and horizontal velocities. Range = 350 m	37
19	MIXED CO. data vs. calculated outrunning vertical and horizontal velocities. Range = 196.6 m	38
20	MIDDLE GUST II data vs. calculated outrunning vertical velocity. Range = 106.7 m	39

LIST OF TABLES

Table		Page
1	DIRECT COURSE and MILL RACE Seismic Data	18
2	MIXED COMPANY Seismic Data	18
3	MIDDLE GUST II and III Seismic Data	20
4	MIDDLE GUST IV Seismic Data	20
5	MISERS BLUFF Seismic Data	21
6	Pre-DICE THROW Seismic Data	21
7	Summary of the Proposed Prediction Procedure for the Outrunning Waveform	40

SECTION 1
INTRODUCTION

One of the major recommendations of the President's Commission on the Modernization of Strategic Forces (Ref. 1) was the development of a land-mobile, small missile. An outgrowth of this recommendation was the hard mobile launcher concept. Because this is a low overpressure threat, the need for an accurate prediction procedure for the outrunning ground shock wave has increased. The outrunning wave, as defined in this report, is the low frequency ground motion that arrives before the airblast. This wave may be due to the energy coupled at ground zero or to the upstream airblast. The objective of this report is to evaluate the accuracy of existing prediction methods for the outrunning waveform and, if necessary, propose a new prediction method.

In the past, the prediction of ground motions induced by High Explosive (HE) and Nuclear Explosive (NE) experiments has been the subject of extensive research. Such ground motions can be characterized as follows: 1) airblast-induced, 2) direct-induced, or 3) upstream-induced. Airblast-induced motions are due to the local airblast at the point of interest. Direct-induced motions result from energy coupled at ground zero. Upstream-induced motions are caused by the upstream airblast.

Depending upon explosive yield, height-of-burst (HOB), and geology, ground disturbances may arrive at the point of interest prior to the airblast (i.e., "outrun" the airblast). These disturbances are direct-induced or upstream-induced in nature. At low yields and deep surface layers, outrunning occurs when the airblast velocity falls below the compressional wave speed of the surface layer. At higher yields, or shallow surface layers, faster underlying layers transmit the ground shock. In these cases, outrunning can occur at relatively high overpressures.

Outrunning in the first layer is shown in Figure 1. As seen in this figure, the outrunning region is subdivided into the transeismic and subseismic regions. In the transeismic region, the P-wave velocity is greater than the airblast velocity, which in turn exceeds the S-wave velocity, i.e.,

$$C_s < U < C_p$$

where:

C_p = P-wave velocity
U = airblast velocity
C_s = S-wave velocity

In the subseismic region, the airblast velocity is less than the S-wave velocity also, i.e.,

$$U < C_s < C_p$$

Outrunning due to the refraction of energy through a faster, underlying zone is shown in Figure 2. Generally, the refracted P-wave generated by the critically incident P-wave travels parallel to the layer interface at the velocity of the lower layer. This wave is the source of head waves which propagate into the surface layer. Head waves due to the energy at the origin are the primary source of the outrunning seen in data.

Several methods exist for the prediction of the ground shock induced by explosions. Airblast-induced ground motions are predicted with reasonable confidence using finite difference and finite element computer codes. Upstream-induced ground motions, which arrive after the airblast, can be predicted using semi-empirical methods (Ref. 2). Several attempts have been made in the past for the prediction of the outrunning motions. The objective of this report is to investigate the methods produced by such attempts and propose a new method for the prediction of the outrunning wave.

The existing outrunning models are investigated in Section II of this report. The development of the new outrunning prediction procedure will be discussed in Section 3. Section 4 lists the conclusions reached in this work.

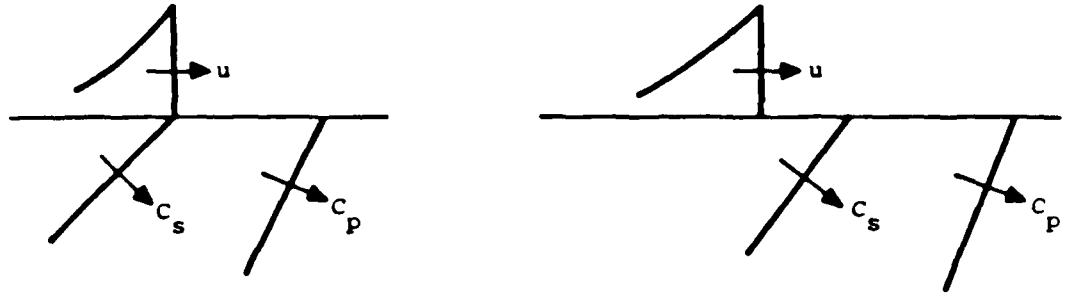

(a) Transseismic Case
$C_s < U < C_p$

(b) Subseismic Case
$U < C_s < C_p$

Figure 1. Surface layer outrunning.

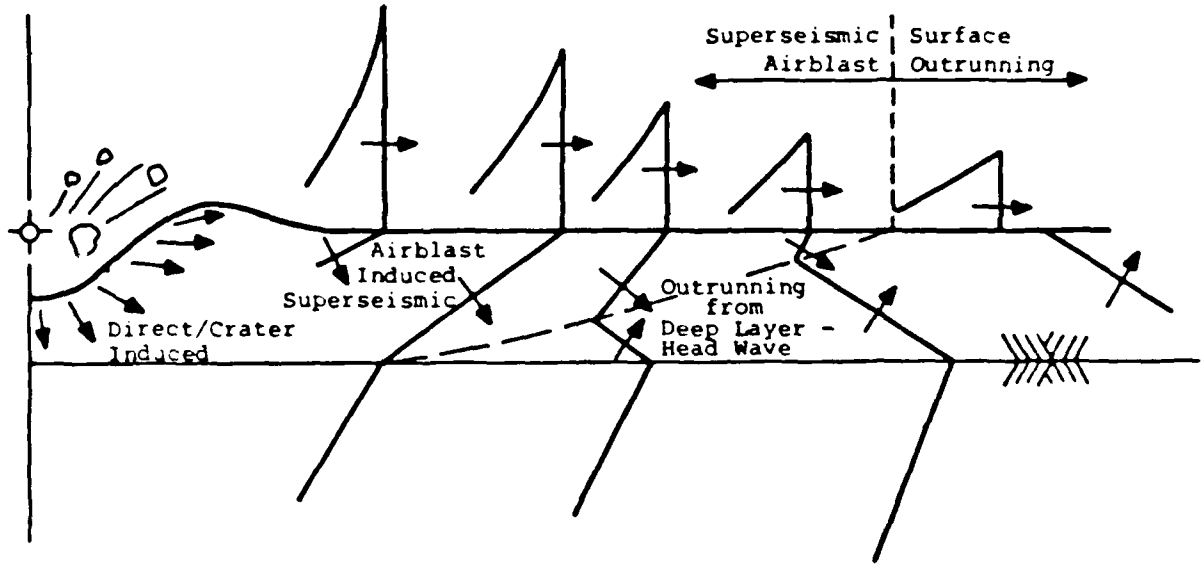

Figure 2. Outrunning due to layer refraction.

SECTION 2
PREVIOUS OUTRUNNING MODELS

Research has been conducted in the past for the theoretical or empirical prediction of the outrunning wave. Four of the methods produced are discussed below.

1) A well-documented method for predicting the entire waveform in the outrunning region (outrunning and upstream-induced that arrive after the airblast) was developed by Sauer (Ref. 3). In this method, a characteristic waveform for the vertical motion was developed using ground motion data obtained from about a dozen surface and above-ground nuclear tests. The data indicated that the period of oscillation increases with range. Thus, a characteristic time, T_2, was introduced as a scaling factor to time. T_2 is a function of range and is defined as follows:

$$T_2 \text{ (msec)} = 100 + 0.82\ \Delta R \text{ (m)} \qquad (1)$$

where:

ΔR = difference between the range of interest and the range at which the first outrunning occurs.

The vertical velocity was normalized with respect to the peak velocity of the waveform (Fig. 3).

Plots from available data provided by DIRECT COURSE, MIXED COMPANY, MILL RACE and other experiments that will be discussed in the next section, indicated that the scaling factors used by Sauer do not collapse the HE data when very different HOBs, yields, and geologies are used. For example, in Figure 4 the curve developed by Sauer is shown with the data from DIRECT COURSE and MIXED COMPANY at the ranges of 466 m and 197m respectively. (The data shown includes only the outrunning portion of the waveform.) As seen, the magnitudes of the outrunning wave are reasonably approximated on the first cycle and overestimated on the second. In addition, the frequency of the MIXED COMPANY wave has been overestimated.

2) A thorough review on the work conducted in the past for the prediction of the outrunning ground motion can be found in Higgins, et al (Ref. 4). Most of this work includes the later time motions (motions that occur after the airblast). A summary

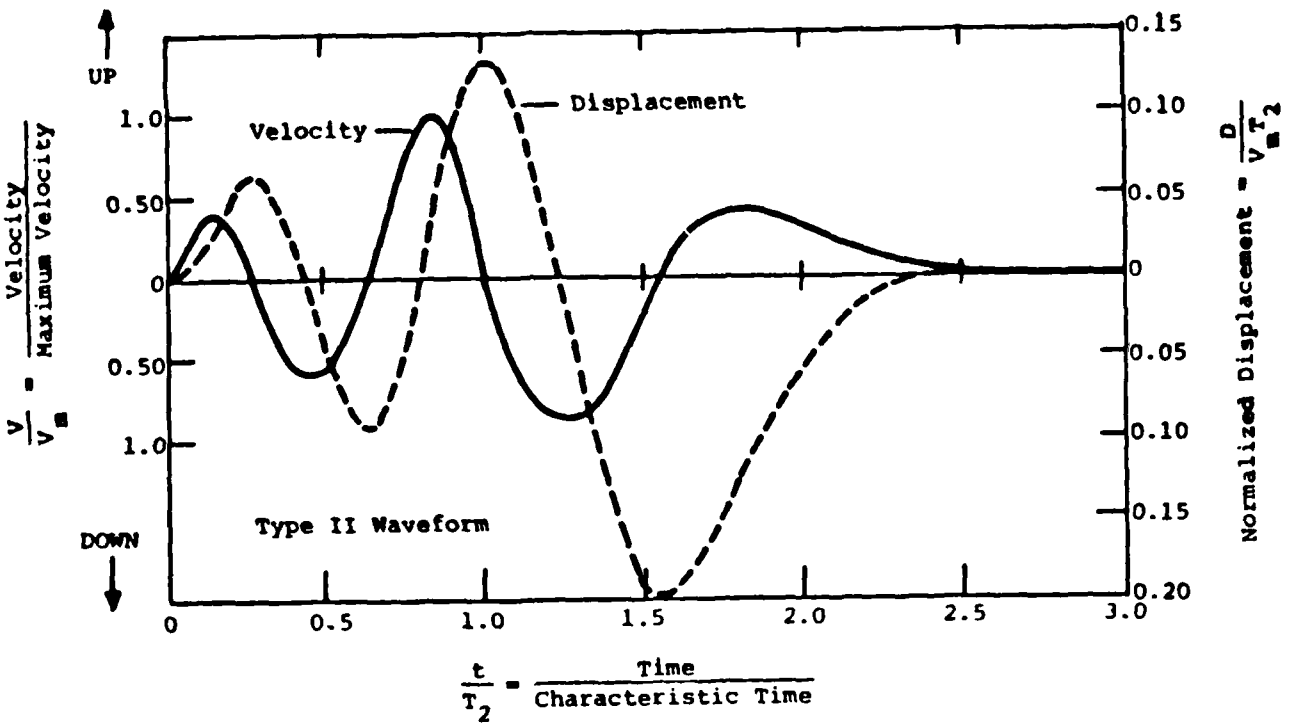

Figure 3. **Outrunning waveform.** (after Sauer et. al, 1964)

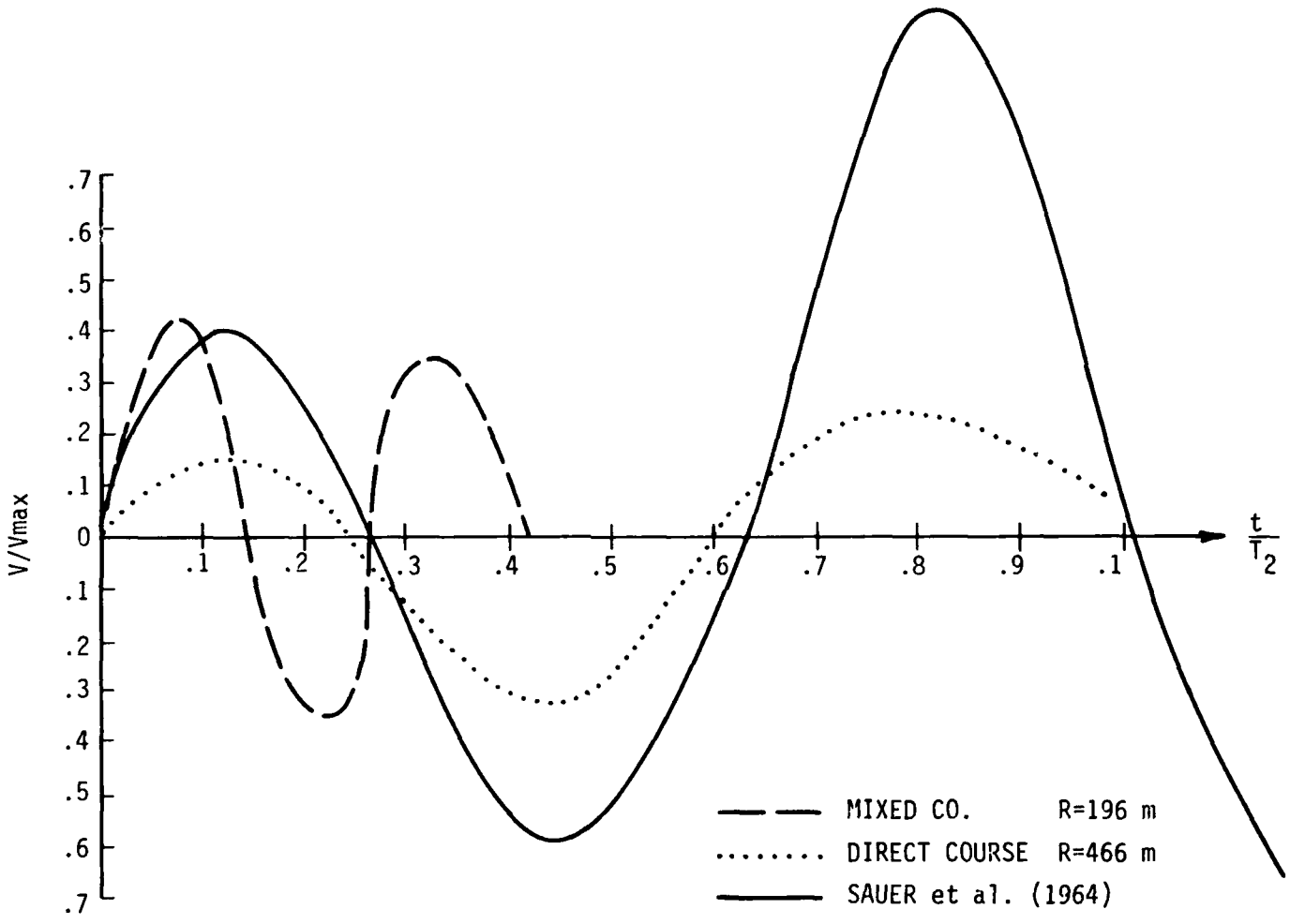

Figure 4. DIRECT COURSE and MIXED COMPANY data compared to the Sauer waveform.

of this work shows the different attempts made in the past toward an understanding of the motions in the outrunning region. A review of several closed form solutions, numerical calculations, and empirical analyses, and the conclusions reached by such works, are included and briefly discussed in this reference.

The empirical analysis developed in Reference 4 involved a characteristic wave of the entire waveform at the outrunning region, which was developed with data provided by MIDDLE GUST II and III and MIXED COMPANY 3. The velocity was normalized by a value V_v, equal to the peak velocity of the upstream-induced waveform in the outrunning region. The time was scaled by a value τ that is defined as follows:

$$\tau = \frac{t - t_o}{t_v - t_o} \qquad \text{for vertical}$$

$$\tau = \frac{t - t_o}{t_h - t_o} \qquad \text{for horizontal} \qquad (2)$$

where:

t = time after detonation
t_o = time of arrival
t_v = time of occurence of the third upward peak
t_h = time of occurence of the first upward peak

The scaling factor

$$\bar{\tau} = \frac{tC_p}{Va^{1/3}} \qquad (3)$$

where:

t = time
C_p = P-wave velocity at a depth below 7.5 m
V_a = crater volume

brings the MIDDLE GUST and MIXED COMPANY horizontal velocity data into good agreement.

Figure 5 shows the data of MIDDLE GUST II, MIXED COMPANY 3 and MILL RACE at distant ranges. As seen in this figure, the frequency from the experiments used to develop the method is closely predicted, while the frequency of MILL RACE is underpredicted. In addition, HOB cases can not be included in this analysis, because a crater volume is used in the scaling.

3) Another method for predicting the total waveform at the outrunning regions is given by Guros (Ref. 5). By analyzing three 100-ton-HE experiments, Guros derived a characteristic waveform, amplitudes, relations for attenuation with range, time of arrival and frequencies. He also gave directions for the prediction of outrunning in dry and wet site geologies. As in the previous reference, this report also refers to the entire waveform and does not concentrate on the outrunning part of it.

4) Finally, the method for the prediction of upstream-induced motions developed by Labreche et al. (Ref. 2) provides an estimate of outrunning motions. The upstream induced motions are made up of two components. These are: 1) the body wave, which travels at P-wave speeds, and 2) the surface wave, which travels at S-wave speeds. The arrival of both components is calculated from critical refraction theory using the source as the origin. The frequency of the body wave motions is governed by the crater volume and the surface wave frequency is governed by the shear properties of the site profile. In general, this method accurately predicts the arrival time of the outrunning motions. The frequency and magnitude, however, are not consistently predicted. This method was developed primarily for use in the superseismic region and therefore was never thoroughly checked in the outrunning region. Furthermore, it is limited to surface bursts and therefore will not allow variations in burst height.

Most of the references cited above concentrate on a limited number of HE experiments, with the exception of the procedure introduced by Labreche et al. (Ref. 2), which was developed primarily for use in the superseismic region, and the procedure introduced by Sauer et al. (Ref. 3), which was

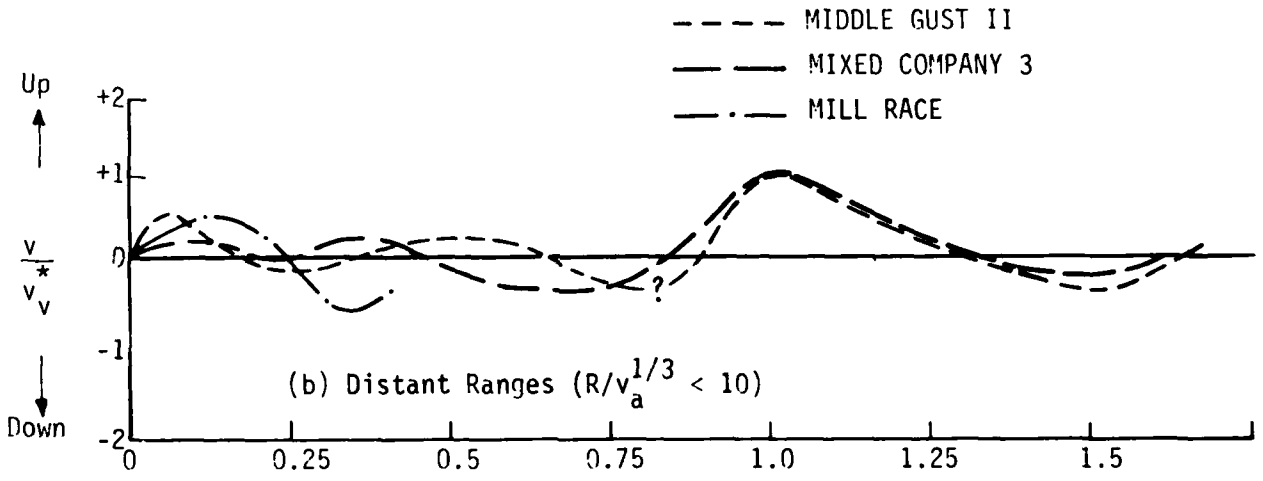

Figure 5. Fits to normalized vertical velocities for various events. (after Higgins et al. 1975)

developed for use in the outrunning region. This second procedure will be used in this report and will be modified using HE data for the prediction of the outrunning portion of the velocity waveform. In Section 3, the development of new scaling factors used in addition to those proposed by Sauer will be presented. Finally, the characteristic waveform shown in Figure 3 will be modified using recent HE data. The waveform produced is general enough to be used for predicting outrunning motions of HE and NE explosions that vary in burst height, geology, and yield.

SECTION 3
DEVELOPMENT OF A CHARACTERISTIC WAVEFORM

The predictior procedure for the outrunning wave proposed by Sauer et al. (Ref. 3) has been chosen to be modified in this report in order to collapse a wide range of data. For this purpose, additional scaling factors were derived for use in conjunction with those proposed by Sauer. These factors are the velocity, V_1, which is the peak velocity of the first cycle of motion in the outrunning region, and an impedance ratio, $[(\rho C_p)\text{rock}/(\rho C_p)\text{soil}]$, of the significant layers in the geology. V_1 was used instead of V_{max} proposed by Sauer, while the impedance ratio was used to multiply the factor t/T_2 (Fig. 3). In this section, the derivation of these factors as well as the data on which they are based are discussed.

Several experiments provide a substantial data base on the outrunning region. Good quality data is provided by DIRECT COURSE (Ref. 6), MILL RACE (Ref. 7), and MIXED COMPANY (Ref. 8). Other sources of limited data are Pre-DIRECT COURSE (Ref. 9), MIDDLE GUST II (Ref. 10), III (Ref. 11), and IV (Ref. 12), MISERS BLUFF (Ref. 13), and Pre-DICE THROW (Ref. 14). This data base includes surface tangent and height of burst explosions, as well as a variety of geologies and yields.

Major emphasis in the empirical analysis of these data was placed on the velocity waveform, because the velocity is more easily interpreted than other motion components. The frequency and magnitude of the waveform were the two major parameters considered. The airblast-induced motion or any motion arriving after the airblast was not considered in this analysis.

3.1. Test Site Geologies

DIRECT COURSE was conducted with 600 T of ANFO (equivalent to 500 T of TNT) exploded at an HOB of 50.6 m. The site geology consisted of clayey sand and sandy clay. A hard caliche layer existed at a depth of 10.6 m. MILL RACE was a similar experiment exploded tangent to the surface on the same geology as DIRECT COURSE. The seismic data of this profile, found in Reference 15, are given in Table 1.

MIXED COMPANY was an experiment conducted with 500 T of TNT exploded tangent to the surface. The site was composed of sandy, clayey silt overlying an intermixed formation of siltstone, sandstone, mudstone and

Table 1. DIRECT COURSE and MILL RACE Seismic Data

(Ref. 15)

H (m)	C_p (m/s)	C_s (m/s)	γ (kg/m^3)
0 - 0.8	365	245	1600
.8 - 3.5	710	545	1696
3.5 - 10.6	900	494	1696
10.6 - 14.6	1325	640	1712
> 14.6	903	470	1792

Table 2. MIXED COMPANY Seismic Data
(Ref. 16)

H (m)	C_p (m/s)	C_s (m/s)	γ (kg/m^3)
0 - 3	655	393	1920
3 - 122	2286	1493	2160

conglomerates. The bedrock consisted of a massive, cross-bedded sandstone. The seismic data of this profile are given in Table 2 (Ref. 16).

MIDDLE GUST II and III were two experiments, each composed of 100 T of TNT, exploded at an HOB of 4.8 m and at surface tangent, respectively. The site was formed by a layer of alluvial sandy clay overlying Cretaceous Pierre shale. A perched water table existed at about 1.2 m. Table 3 contains the seismic data of this site (Ref. 16).

MIDDLE GUST IV consisted of 100 T of TNT detonated at surface tangent. The site overburden was made up of a very thin layer of clayey top soil overlying a layer of silty clay shale and finally a competent clay shale bedrock. This site had a deep water table, unlike that of MIDDLE GUST II and III. The seismic information is contained in Table 4 (Ref. 16).

MISERS BLUFF was an experiment consisting of 120 T of ANFO (equivalent to 100 T of TNT) exploded at surface tangent. The site profile was composed of wind blown silt, clayey silt, and beds of alternating sand and sand gravel. The bedrock consisted of conglomerate sandstone. The seismic data of this site are found in Table 5 (Ref. 16).

Pre-DICE THROW was an experiment consisting of 100 T of TNT exploded at surface tangent. The site geology had layers of silty clay, fine and course silt, and sand with gravel. The seismic data are found on Table 6 (Ref. 16).

3.2. Time of Arrival

The range (or time) at which outrunning first occurs can be found using the airblast arrival time, and the standard seismic velocities and layer depths of the site (Ref. 17). Figure 6 shows the relationship between the times of arrival of the upstream-induced or direct-induced ground motion and the airblast. The point at which the two curves intercept is the range (or time) at which outrunning first occurs.

As seen in this graph, the first outrunning is due to upstream airblast. However, observations from the data indicate that the time of arrival of the first outrunning coincides with the arrival of the critically refracted P-wave from the origin. This apparent inconsistency

Table 3. MIDDLE GUST II and III Seismic Data

(Ref. 16)

H (m)	C_p (m/s)	C_s (m/s)	γ (kg/m^3)
0 - 2.13	610	122	2082
2.13 - 4.57	1768	183	2082
4.57 - 38	2408	1036	2370

Table 4. MIDDLE GUST IV Seismic Data
(Ref. 16)

H (m)	C_p (m/s)	C_s (m/s)	γ (kg/m^3)
0 - 3.0	335	168	2000
3.0 - 7.6	731	260	2160
7.6 - 15.0	1981	457	2368

Table 5. MISERS BLUFF Seismic Data
(Ref. 16)

H (m)	C_p (m/s)	C_s (m/s)	γ (kg/m^3)
0 - 1	335	213	1600
6.1 - 12.2	518	260	1760
12.2 - 43	1707	305	1920

Table 6. PRE-DICE THROW Seismic Data
(Ref. 16)

H (m)	C_p (m/s)	C_s (m/s)	γ (kg/m^3)
0 - 2.4	366	168	1600
2.4 - 33	1877	204	1760
33 - 366	1981	603	1920

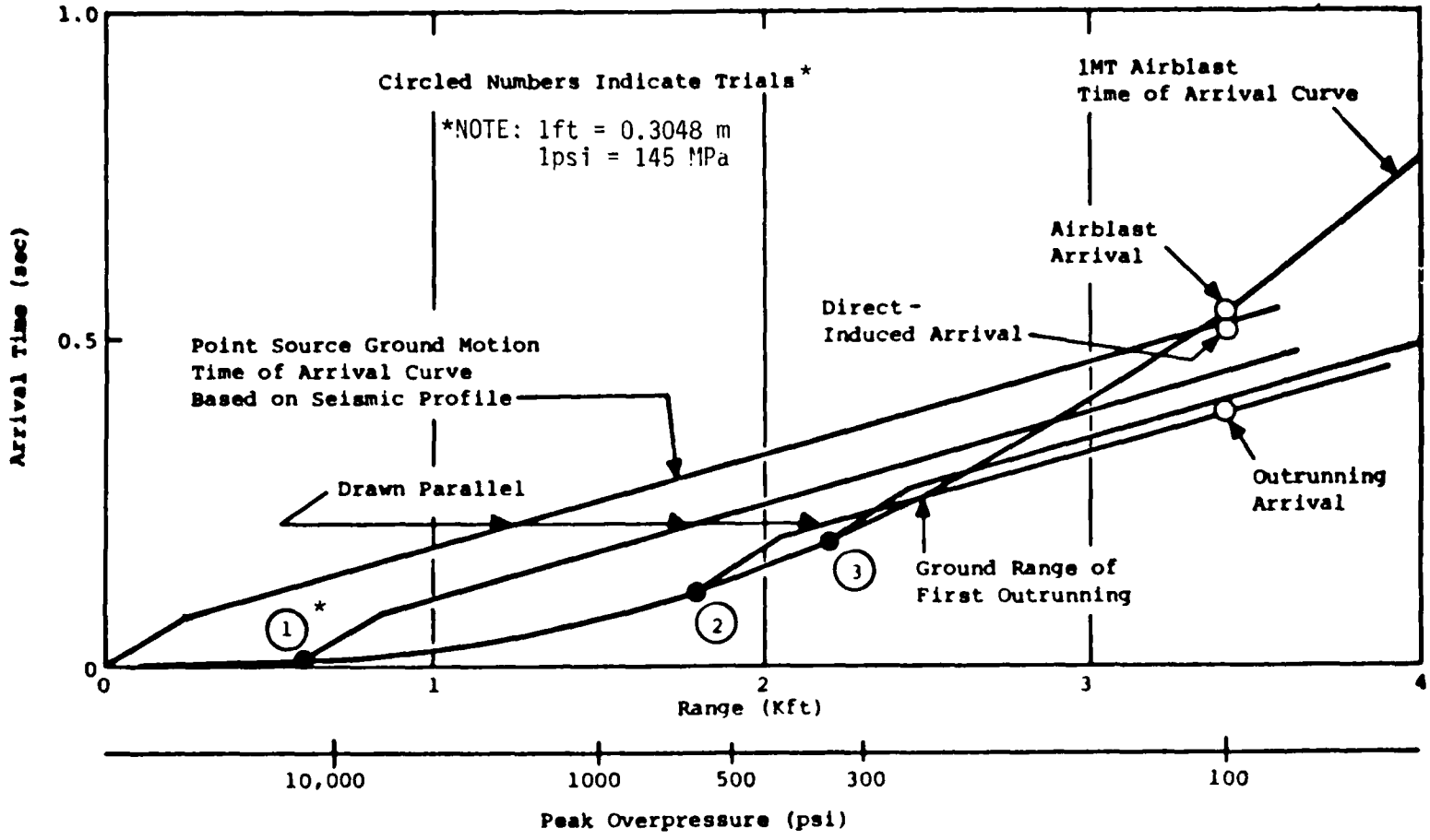

Figure 6. Prediction of the ground shock arrival based on the site geology.

is due to the fact that upstream induced motions are not of sufficient magnitude to create very strong oscillations and, therefore, they are not observed in the data. By the time the direct-induced head waves arrive from the origin, the upstream-induced and the direct-induced waves superimpose to produce the relatively strong oscillation observed in the data.

3.3. Velocity Scaling Factor

To scale the velocity, V, of the waveform, a value, V_1, equal to the value of the first peak of the outrunning wave was used. Figures 7 and 8 show the vertical and horizontal relations of this value with range (scaled to yield) at different depths of several experiments. (The values at different depths fall within the scatter of the data.) The equations that describe the two lines are:

$$V_1 = 2.70(10^6)R^{-2.24} \qquad \text{for Vertical}$$

$$V_1 = 1.26(10^7)R^{-2.37} \qquad \text{for Horizontal} \qquad (4)$$

where R = range in $(m/MT_{NE}^{1/3})$ and V_1 is given in m/s

3.4. Time Scaling Factor

As seen previously (Fig. 4), the frequencies of the waveforms provided by DIRECT COURSE and MIXED COMPANY were very different. DIRECT COURSE was accurately predicted by the curve developed by Sauer (Ref. 3), while MIXED COMPANY was overpredicted. To find the factors that influence the frequency, parametric studies were performed using the CAGGS computer code developed by Britt (Ref. 18). The parameters studied were 1) the depth of the overburden, H, and 2) the impedance ratio between the soil and the rock (or hard layer). As will be seen, the impedance ratio influences the frequency considerably.

The theory in CAGGS is based on the exact Cagniard elastic formulation of the wave propagation theory (Ref. 19). The Cagniard solution was extended by Britt to model the ground shock propagation and motions produced by airburst explosions. The air-earth environment was

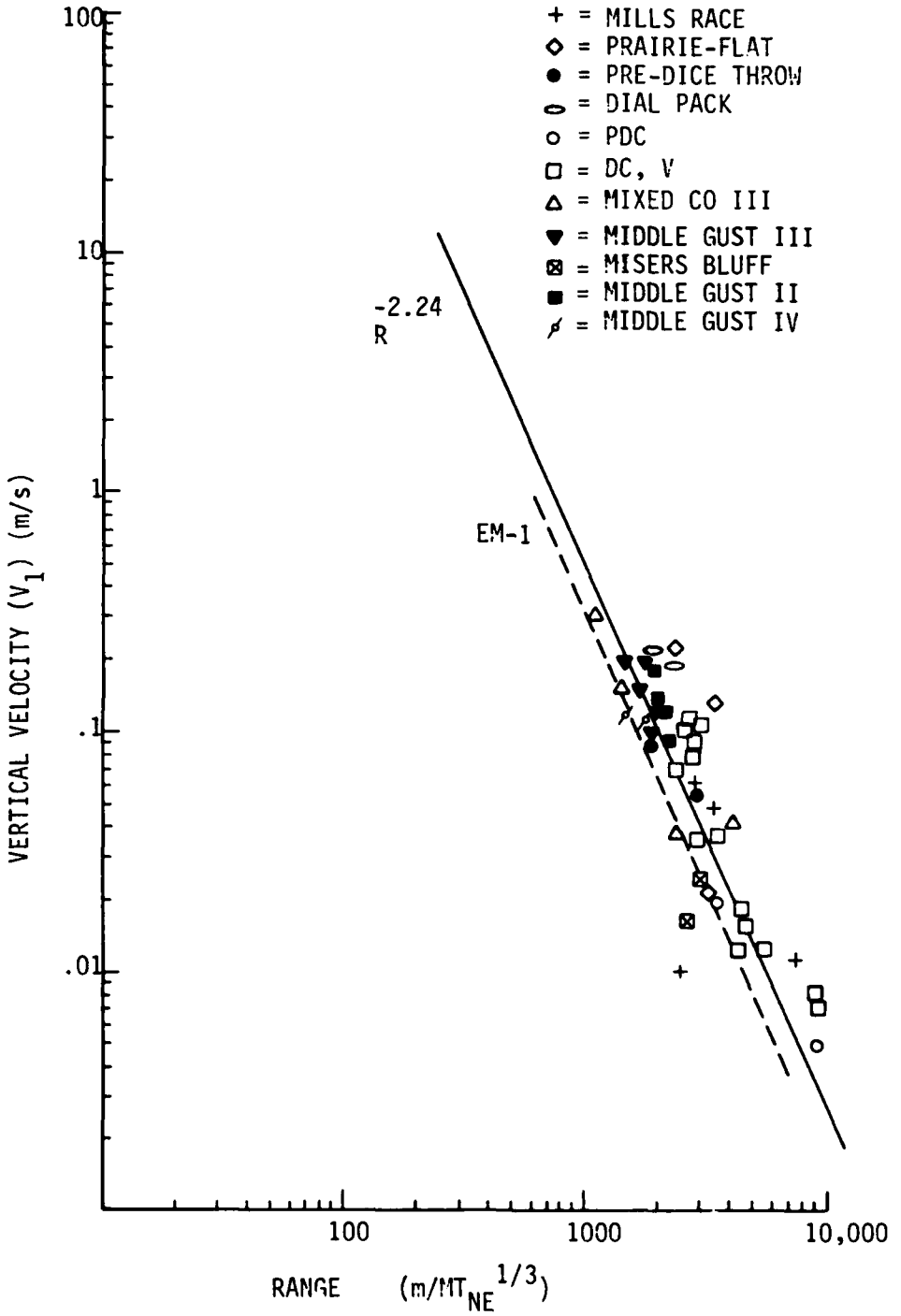

Figure 7. First peak of the outrunning wave vs. range-vertical

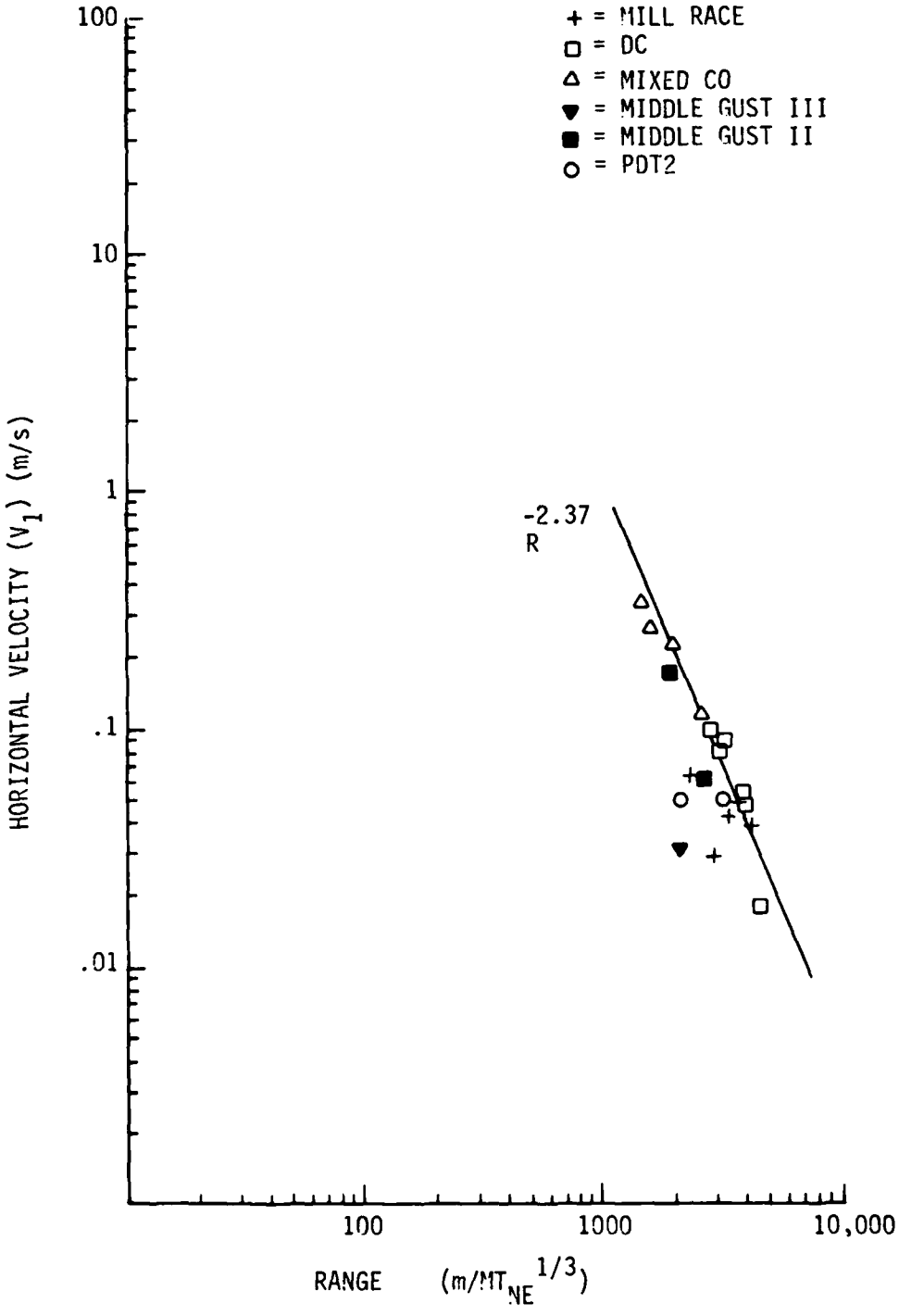

Figure 8. First peak of the outrunning wave vs. range-horizontal.

treated as three elastic layers (air, soil and rock). The explosion was replaced by a point source in an elastic fluid. The airblast was estimated empirically and was used as a source input. The CAGGS solution includes particle velocity waveforms. An example of such results is shown in Figure 9, in which the theoretical results are compared to DIRECT COURSE data at a range of 305 m. As seen in this figure, the comparison between the data and a closed form solution is good. The problem develops at large ranges where the elastic solution underestimates the magnitude of the outrunning motions considerably, and fails to estimate the frequency. CAGGS was used at small ranges for parametric studies to single out the factors that influence the outrunning wave.

Using CAGGS, the vertical and horizontal velocity of MIXED COMPANY at a range of 196 m were calculated and shown in Figure 10. As shown in Table 2, the depth to the rock in the site of this experiment is equal to 3 m. Figure 11 shows the vertical and horizontal velocity of the same profile when the depth to the rock was changed to 5.8 m. Observation of these curves reveals that the depth to the rock does not influence the shape of the horizontal velocity waveform. However, the vertical velocity shows a dependence to the depth of the softer layer. The shape of the waveform changed and the frequency was affected. The magnitude of the first peak in both the vertical and horizontal waves remained unchanged.

However, the factor that seemed to influence considerably both the vertical and the horizontal waveforms is the impedance ratio between the soil and the rock of the site. The impedance of each material was calculated using the density, ρ, and the P-wave speed, C_p, of the material. Figure 10 shows the calculated particle velocity of MIXED COMPANY at a range of 196 m and a rock velocity of 2286 m/sec (the impedance ratio is equal to 3.9). Figure 12 shows the velocity waveform of the same experiment when the P-wave speed of the rock was reduced to 1524 m/sec (the impedance ratio is equal to 2.88). When the impedance was increased to 5.78, its influence on the outrunning wave became even more noticeable (Fig. 13). A considerable change seems to occur in the frequency and general shape of both the vertical and the horizontal waves. Consequently, the impedance ratio was used, along with the characteristic time T_2, as a scaling ratio in the derivation of a characteristic wave.

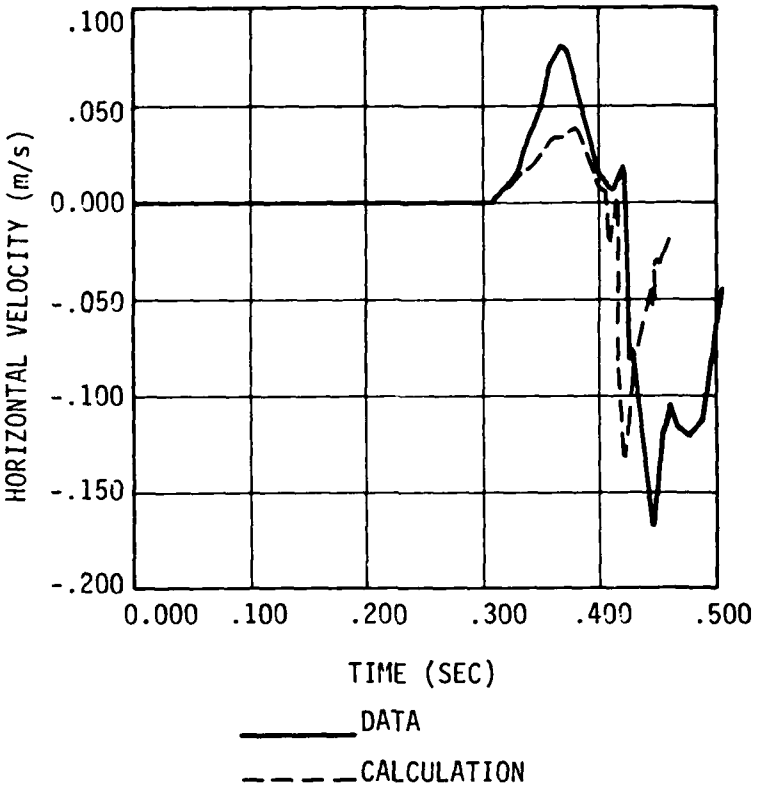

Figure 9. DIRECT COURSE data vs. calculated outrunning ground motion (range = 305 m)

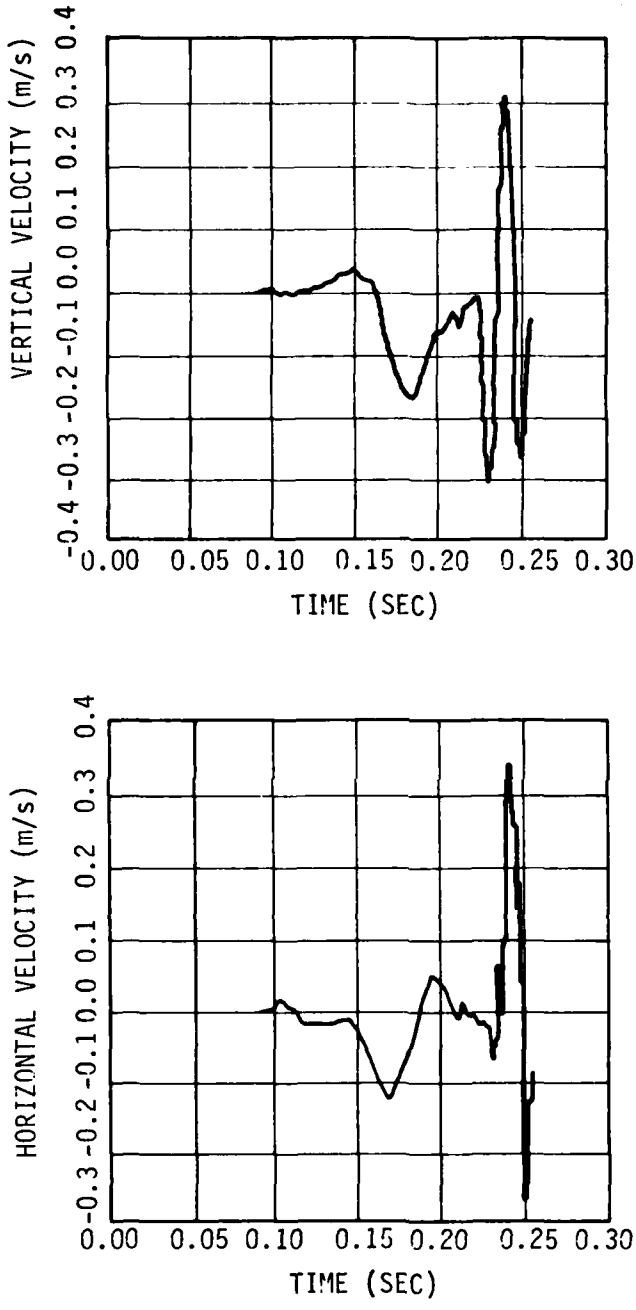

Figure 10. Calculated vertical and horizontal velocities with CAGGS--MIXED CO., range = 196 m, depth = 2.7 m, impedance ratio = 3.9

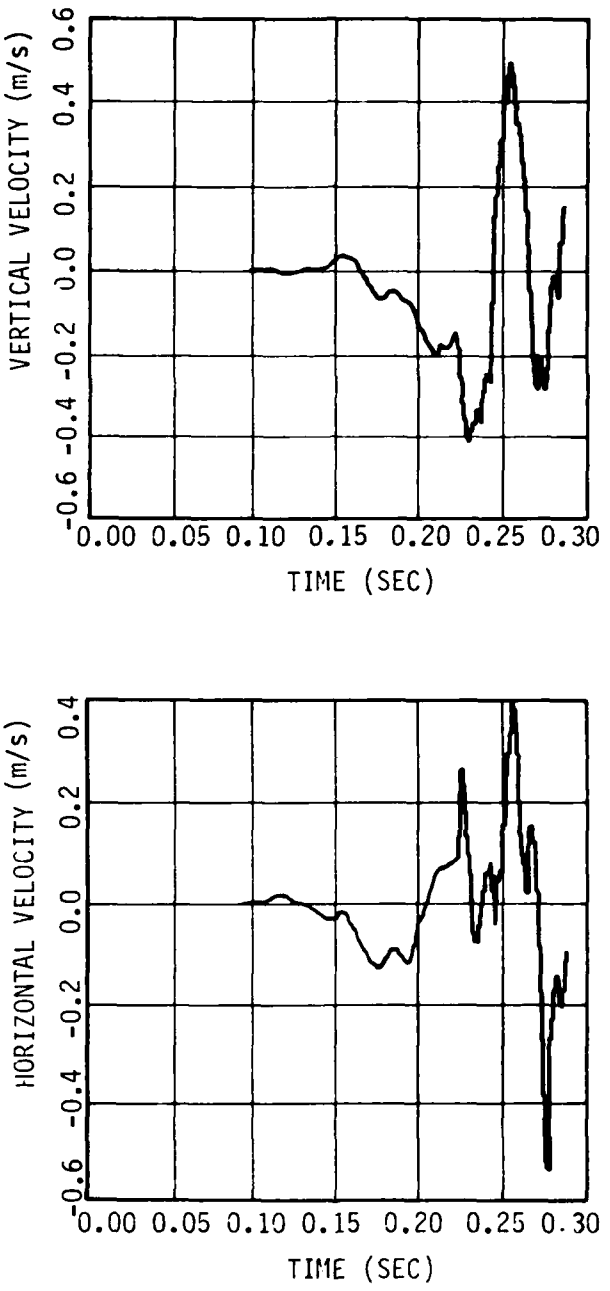

Figure 11. Calculated vertical and horizontal velocities with CAGGS--MIXED CO., range = 196 m, depth = 5.8 m

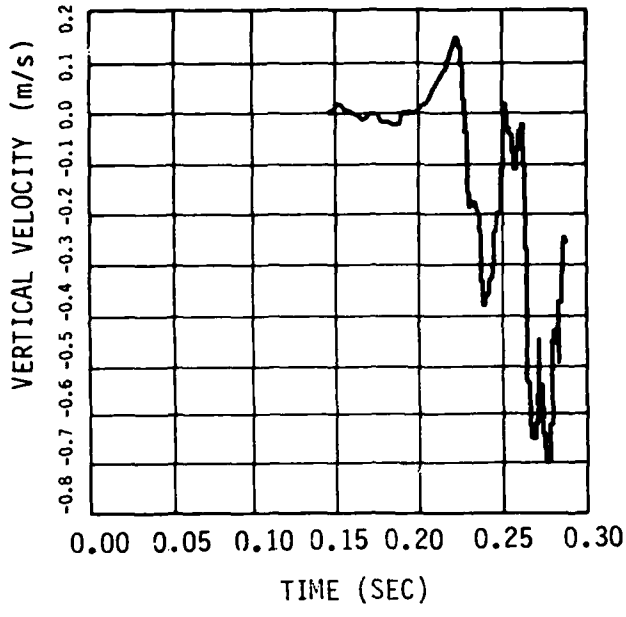

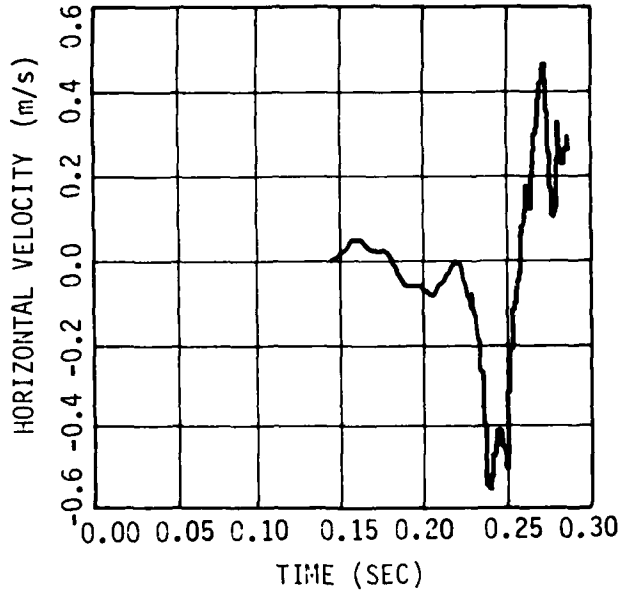

Figure 12. Calculated vertical and horizontal velocities with CAGGS--MIXED CO., range = 196 m, depth = 2.7 m, impedance ratio = 2.38

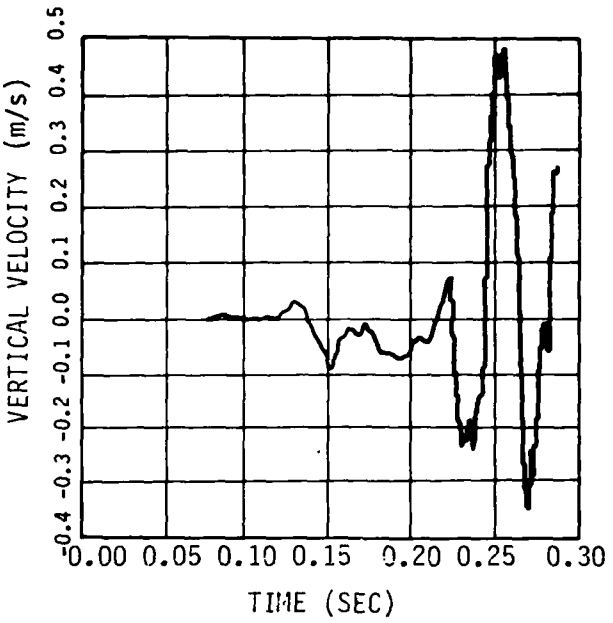

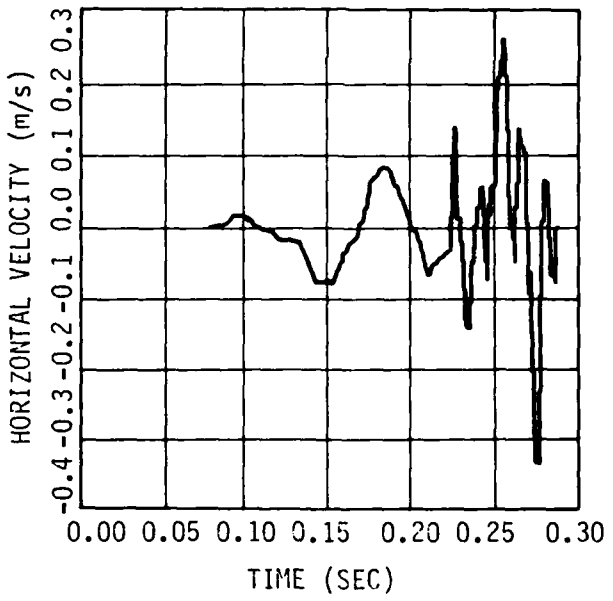

Figure 13. Calculated vertical and horizontal velocities with CAGGS--MIXED CO., range = 196 m, depth = 2.7 m, impedance ratio = 5.78

It should be noted here that the largest impedance ratio between the layers of the site should be used. This could be between the soil and the rock, the soil and the water table, or two layers of soil. At any layer interface at which the impedance ratio is calculated, the weighted average of the properties above this layer must be used.

3.5. Characteristic Wave

Using the new scaling factors, (V_1 and the impedance ratio), the outrunning waveforms from DIRECT COURSE, MILL RACE, MIXED COMPANY, MIDDLE GUST II, III, and IV, MISERS BLUFF, and Pre-DICE THROW were plotted in the normalized fashion as shown in Figure 14. A characteristic waveform was then derived by averaging this data. The vertical and horizontal waveforms that were derived are shown in Figures 15 and 16.

The characteristic waveform that was derived in this study was programmed into the Wave Synthesis Model (WSM) computer code. Several examples were prepared to show its comparison to data.

Figures 17 through 20 show the vertical and horizontal comparisons of the data with the calculations performed using WSM. The tests used in these comparisons are DIRECT COURSE, MILL RACE, MIXED COMPANY, and MIDDLE GUST II. The ranges at which the comparisons are made are at the outrunning regions; the depths are all shallow. As seen, both the magnitudes and the frequencies of these experiments are very closely predicted. The DIRECT COURSE (Fig. 17) comparison includes the entire waveform at a range of 466 m. This prediction procedure produced vertical and horizontal waveforms with an average error of 17 percent in magnitude and 5 percent in frequency. The other waveforms show the outrunning component only. MILL RACE (Fig. 18), at the range of 350 m, was predicted with an average error of 12 percent in magnitude and 12 percent in frequency. MIXED COMPANY (Fig. 19), at the range of 196 m, was predicted with an average error of 23 percent in magnitude and 8 percent in frequency. Finally, MIDDLE Gust II (Fig. 20), at the range of 107 m, had an average of 12 percent error in magnitude and 9 percent error in frequency in the predicted wave form. (NOTE: The experiments used to evaluate the procedure were those used to derive it. The procedure should be evaluated again as new outrunning data becomes available.)

A summary of the proposed prediction procedure is given in Table 7.

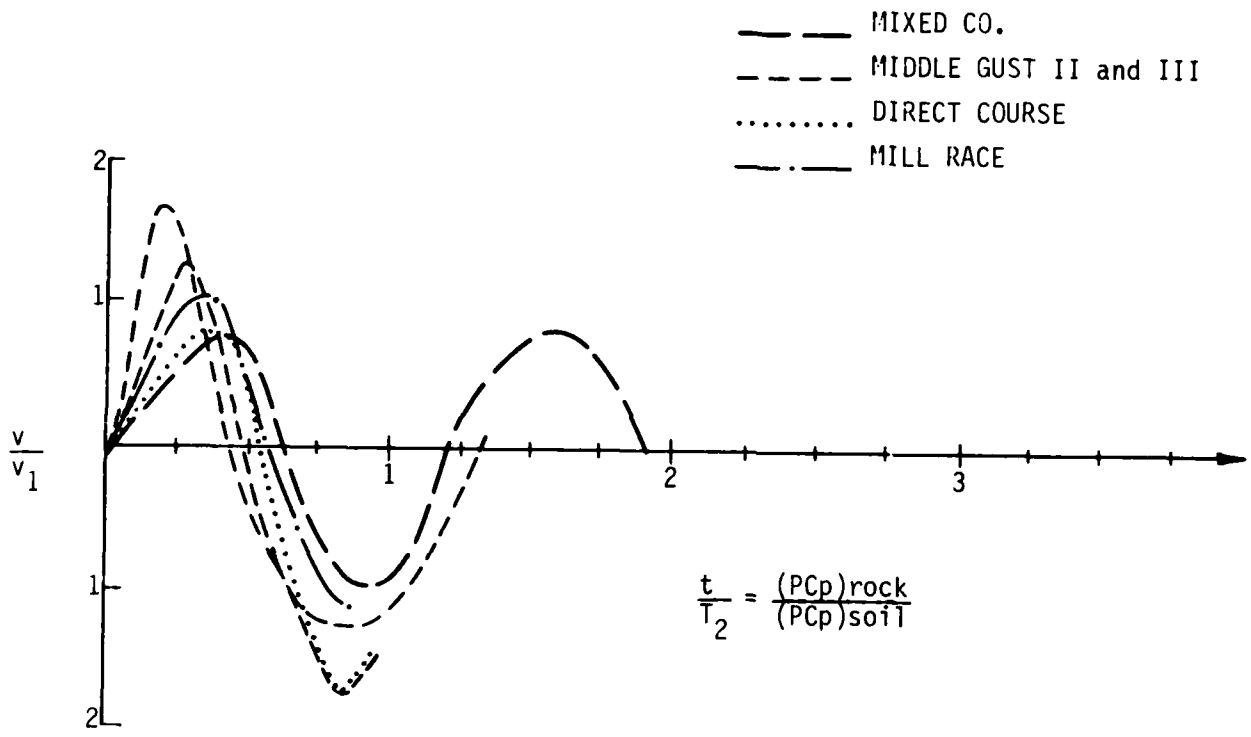

Figure 14. Different data plotted with the new scaling factors.

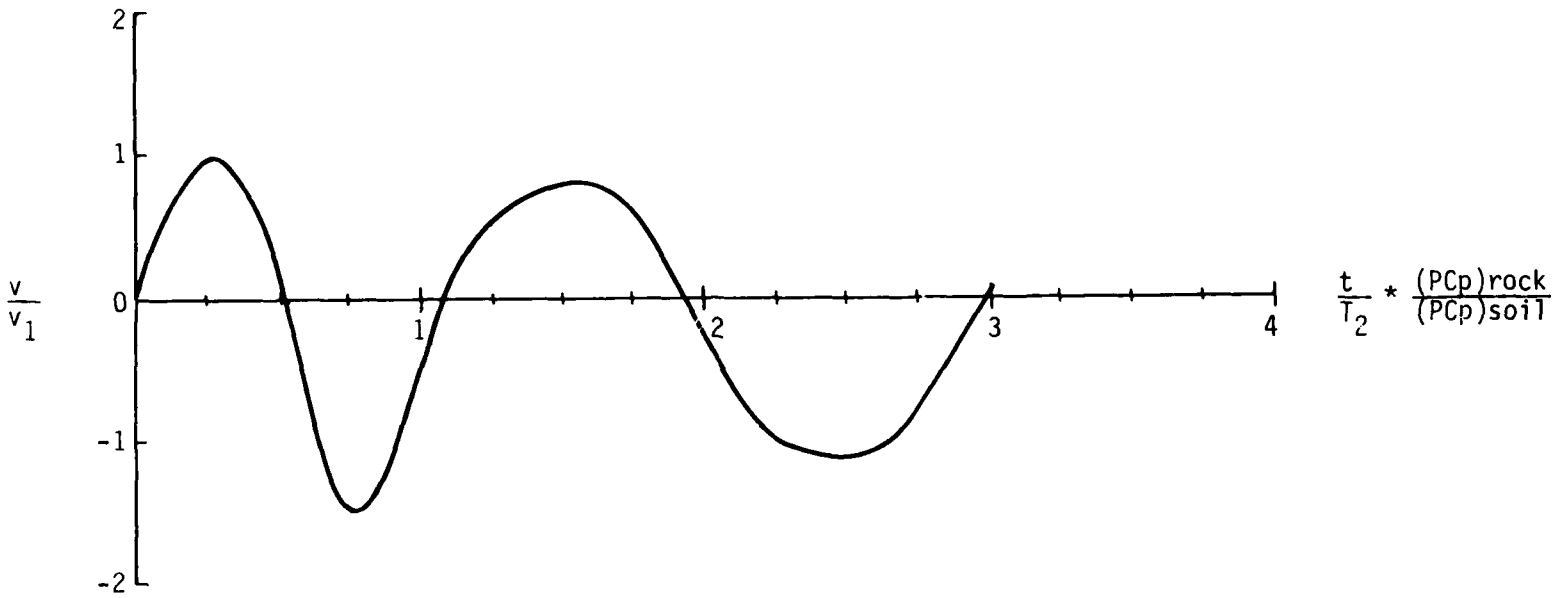

Figure 15. Characteristic vertical velocity waveform.

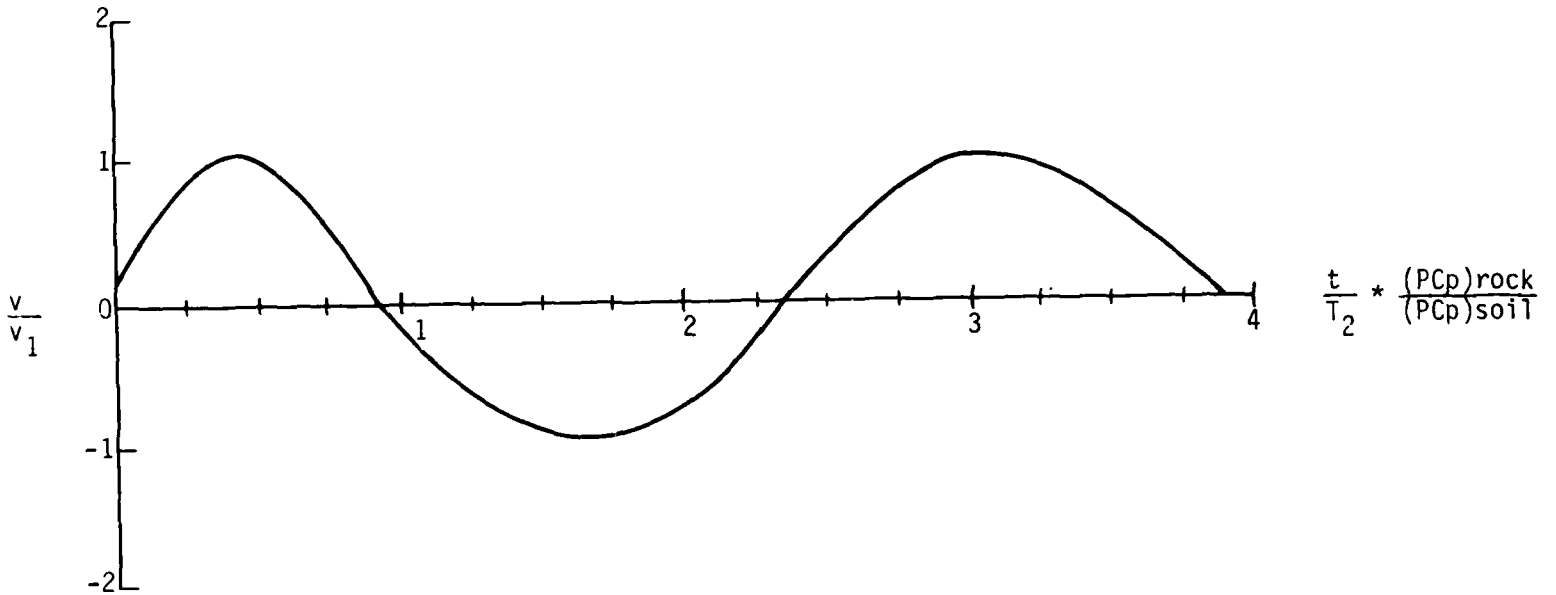

Figure 16. Characteristic horizontal velocity waveform.

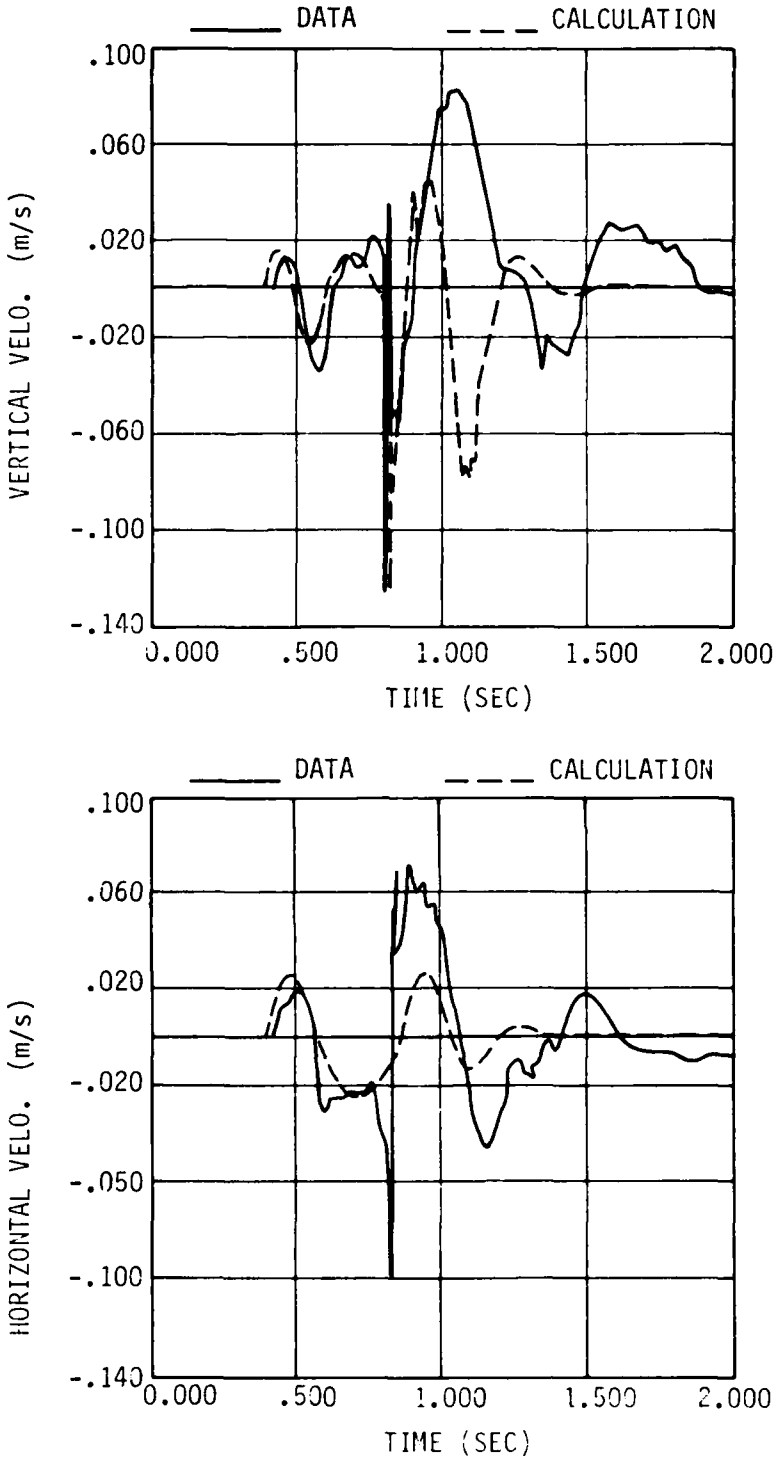

Figure 17. DIRECT COURSE data vs. calculated vertical and horizontal velocities. Range = 466 m

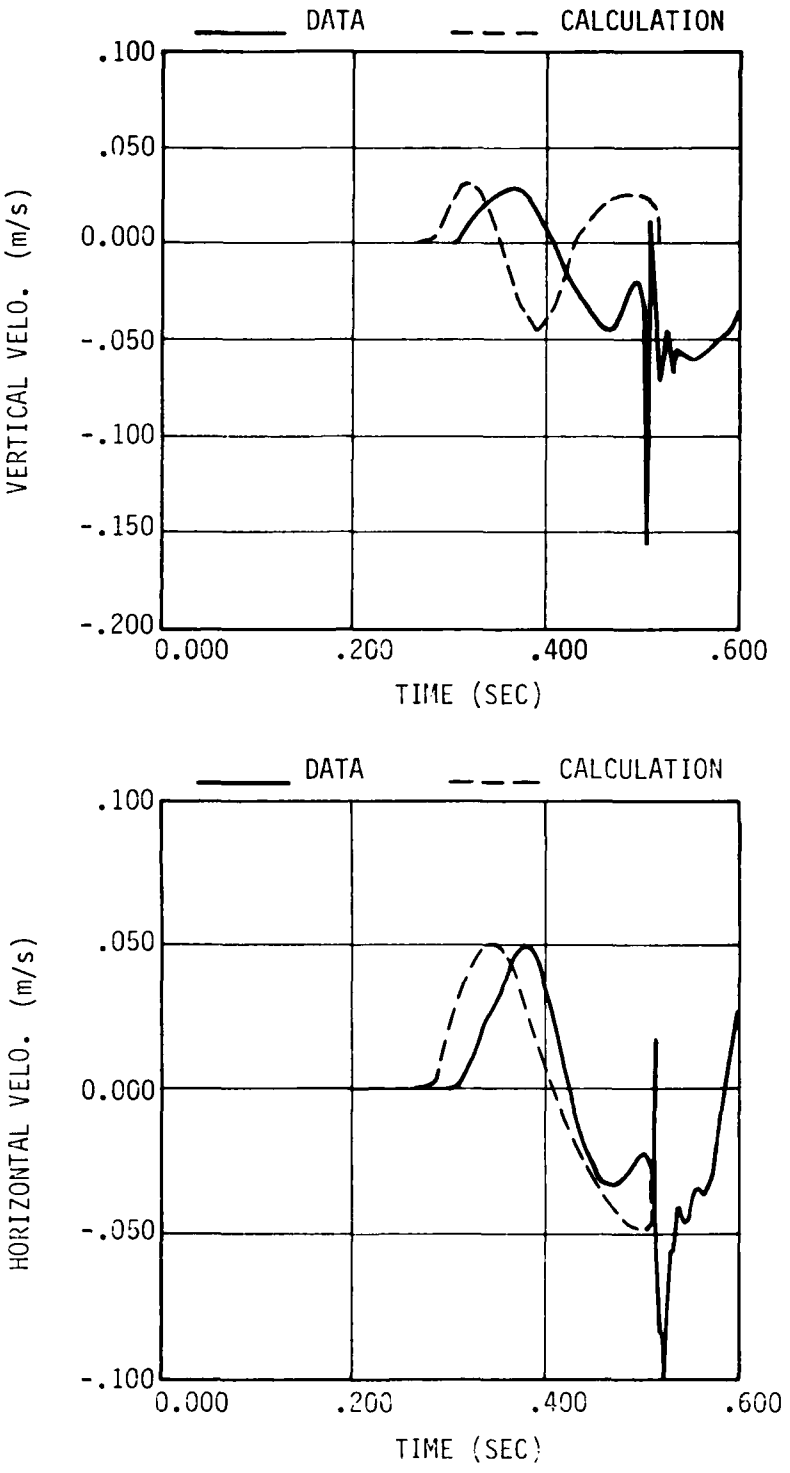

Figure 18. MILL RACE data vs. calculated outrunning vertical and horizontal velocities. Range = 350 m

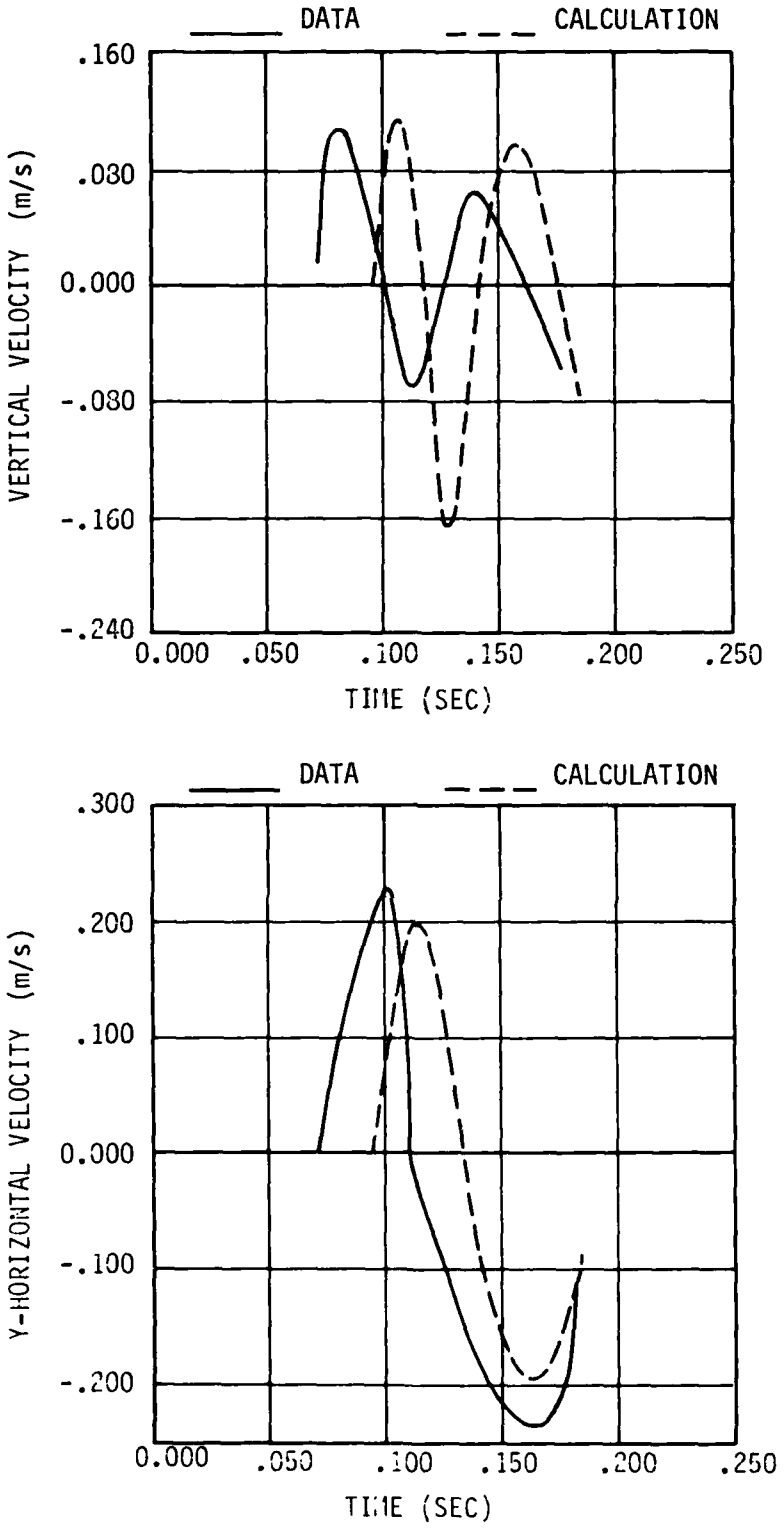

Figure 19. MIXED CO. data vs. calculated outrunning vertical and horizontal velocities. Range = 196.6 m

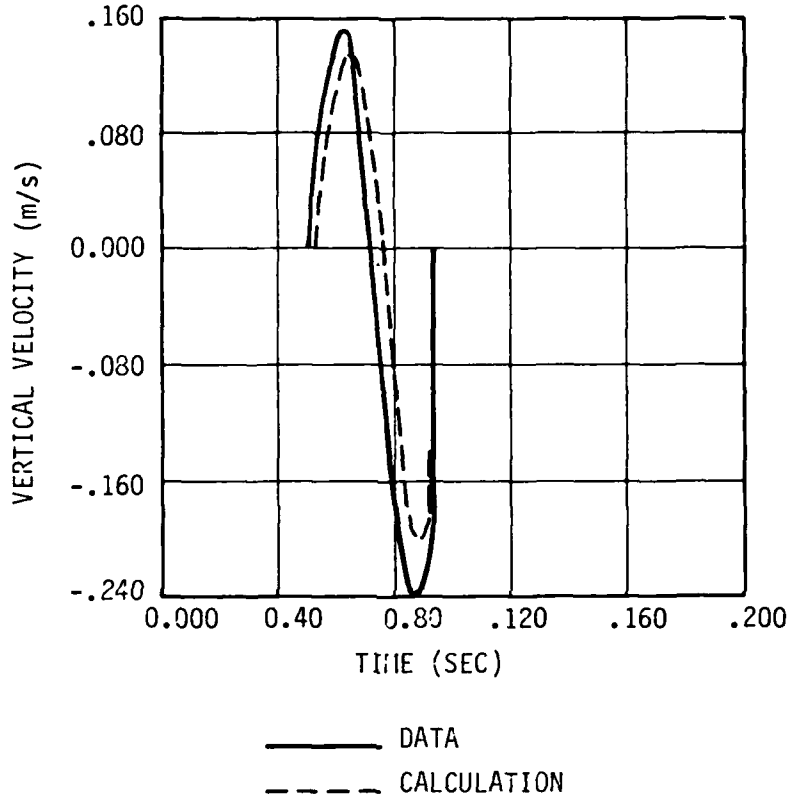

Figure 20. MIDDLE GUST II data vs. calculated outrunning vertical velocity. Range = 106.7 m

Table 7. Summary of the proposed prediction proceudre for the outrunning waveform.

1) Time of arrival and duration--Time of arrival of the outrunning wave is calculated using the standard seismic velocities and layer depths of the site. In multilayered sites, it can be found using the following equation:

$$t_a(n) = \left(\sum_{i=1}^{n} 2H_i \sqrt{\frac{1}{C_1^2} - \frac{1}{C_{n+1}^2}} \right) + \frac{x}{C_{n+1}} + TABO$$

where

$t_a(n)$ = arrival time of head wave from n^{th} interface

H_i = thickness of the i^{th} layer

C_i = compression wave velocity in the i^{th} layer

C_{n+1} = compression wave velocity in the $(n+1)^{th}$ layer

TABO = time of arrival of the airblast at the origin (for HOB explosions only)

2) Scaling factors--The velocity is scaled with a factor, V_1, equal to the peak velocity of the first cycle in the outrunning regions. V_1 is given in m/sec and is calculated as follows:

$V_1 = 2.70\ (10^6)\ R^{-2.24}$ for vertical velocities

$V_1 = 1.26\ (10^7)\ R^{-2.37}$ for horizontal velocities

where: R = range of interest in $m/MT^{1/3}_{NE}$

The time is scaled with two factors:

a) a characteristic time, T_2, where

$T_2(sec) = 100 + 0.82\ \Delta R(m)$

in which ΔR is the difference in range between the point of interest and the point of the first outrunning.

Table 7. Summary of the proposed prediction procedure for the outrunning waveform (Continued).

b) an impedance ratio,

$(\rho C_p)rock/(\rho C_p)soil$

The time scaling factor tf is equal to

$$tf = \frac{t}{T_2} * \frac{(\rho C_p)rock}{(\rho C_p)soil}$$

in which t is zero at the time of arrival of the outrunning wave.

3) Waveform prediction--The waveform is predicted up to the time of arrival of the airblast. After that point other prediction procedures can be used. The following equations describe the waveforms of Figures 15 and 16:

Vertical

$$V_V = V_1\ (1)\ \sin\left(\frac{\pi}{.525}\right)tf \qquad \text{for } 0 < tf < .525$$

$$V_V = V_1\ (-1.5)\ \sin\left(\frac{\pi}{.55}\ (tf - .525)\right) \qquad \text{for } .525 < tf < 1.075$$

$$V_V = V_1\ (.85)\ \sin\left(\frac{\pi}{.85}\ (tf - 1.075)\right) \qquad \text{for } 1.075 < tf < 1.925$$

$$V_V = V_1\ (-1.1)\ \sin\left(\frac{\pi}{1.075}\ (tf - 1.925)\right) \qquad \text{for } tf > 1.925$$

Horizontal

$$V_H = V_2\ (1)\ \sin\left(\frac{\pi}{0.9}\right)tf \qquad \text{for } 0 < tf < 0.9$$

$$V_H = V_2\ (-1)\ \sin\left(\frac{\pi}{1.5}\ (tf - 0.9)\right) \qquad \text{for } tf > 0.9$$

SECTION 4

CONCLUSIONS AND RECOMMENDATIONS

4.1. Conclusions

By the empirical analysis and the numerical calculation, several conclusions were reached.

1) First arrivals in the outrunning region are due to head waves from underlying layers and coincide with the P-wave arrival from the burst point.

2) The first peaks of the outrunning waves attenuate at a rate of $R^{-2.24}$ for vertical and $R^{-2.37}$ for horizontal waves. Since they are produced by the headwave generated at the hard layer, they do not attenuate with depth. The magnitudes of the first peaks at depth fall within the scatter of the data with those at surface.

3) Height-of-burst does not influence the outrunning wave significantly.

4) Depth to the hard layer influences the magnitude and frequency of the vertical outrunning wave only.

5) The impedance ratio between the soil and rock of the site strongly influences the frequency and magnitude of the vertical and horizontal outrunning waves.

6) The magnitude and period of the horizontal outrunning wave are larger than those of the vertical wave

4.2. Recommendations

As data becomes available, it should be used to enrich the data base of this study and reduce the uncertainties associated with this prediction procedure.

REFERENCES

1 Scowcroft, B., "Report of the President's Commission on Strategic Forces," Office of the Secretary of Defense, Washington, D.C., April 1983.

2 Labreche, D.A., et al., Updated Ground Shock Prediction Techniques for EM-1, Draft final report on Contract DNA001-80-C-0212, Applied Research Associates, Albuquerque, New Mexico (27 April 1984).

3 Sauer, F.M., Clark, G.B., and Anderson, D.C., "Part Four--Empirical Analysis of Ground Motion and Cratering," Nuclear Geoplosics, DASA-1285 (IV), Defense Atomic Support Agency, Washington, D.C. (May 1964).

4 Higgins, C.J., and Schreyer, H.L., An Analysis of Outrunning Ground Motions, AFWL-TR-74-220, Kirtland AFB, New Mexico (May 1974).

5 Guros, F., Predictions of Oscillatory Ground Motions for 100-Ton High Explosive Single Burst at Missile-X Type Sites, AFWL-TR-79-107, Kirtland AFB, New Mexico (July 1980).

6 Ingram, J.K., DIRECT COURSE Data, Department of the Army, Waterways Experiment Station, Corps of Engineers, Vicksburg, Mississippi (February 1984).

7 Reid, G.H., and Grayson, R.M., Proceedings of the MILL RACE Preliminary Results Symposium, 16-18 March 1982, Volume 1, Test Directorate, Field Command, DNA, Kirtland AFB, New Mexico (July 1982).

8 Ingram, J.K., MIDDLE NORTH Series MIXED COMPANY Event Ground Shock from a 500-ton High Explosive Detonation on Soil near Sandstone, U.S. Army Engineer Waterways Experiment Station, Weapons Effects Laboratory, Vicksburg, Mississippi (August 1975).

9 Ingram, J.K., Ground Motion Measurements Pre-DIRECT COURSE Event, Department of the Army, Waterways Experiment Station, Corps of Engineers, Vicksburg, Mississippi (December 1982).

10 MIDDLE GUST II, Free-field Data Report, EG&G Report AL-831-2 for the Air Force Weapons Laboratory under Contract AF29601-71-C-0100, EG&G, Inc., Albuquerque, New Mexico (March 1973).

11 MIDDLE GUST III, Free-field Data Report, EG&G Report AL-831-3 for the Air Force Weapons Laboratory under Contract AF29601-71-C-0100, EG&G, Inc., Albuquerque, New Mexico (February 1973).

REFERENCES
(concluded)

12 MIDDLE GUST IV, Free-field Data Report, EG&G Report AL-831-4 for the Air Force Weapons Laboratory under Contract AF29601-71-C-0100, EG&G, Inc., Albuquerque, New Mexico (May 1973).

13 Murrell, D.W. and Stout, J.H., MISERS BLUFF Series; Phase II, Ground Shock and Airblast Measurements Data Report, Structures Laboratory, U.S. Army Engineer Waterways Experiment Station, Vicksburg, Mississippi (March 1979).

14 Murrell, D.W., DICE THROW Series, Pre-DICE THROW II Event, Event 1, U.S. Army Engineer Waterways Experiment Station, Vicksburg, Mississippi (July 1977)

15 Phillips, J.S. and Hassiotis, S., Development of an Empirical Procedure for the Prediction of Ground Motions from a Height-of-Burst Explosion, Applied Research Associates, Albuquerque, New Mexico (November 1984).

16 Higgins, C.J., Errata sheet on Elastic Profiles for High Explosive Test Sites, University of New Mexico, Civil Engineering Research Facility (August 1978).

17 Sauer, F.M., "Ground Motion Produced by Above Ground Nuclear Explosions," AFSWC-TDR-59-71, Air Force Special Weapons Center, Kirtland AFB, New Mexico (1959).

18 Britt, J.R., Calculation of Ground Shock Motion Produced by Airblast Explosions Using Cagniard Elastic Propagation Theory, Structures Laboratory, U.S. Army Engineer WES, Vicksburg, Mississippi (September 1980).

19 Cagniard, L., Reflection and Refraction of Progressive Seismic Waves, McGraw-Hill, New York (1962).

DISTRIBUTION LIST

DEPARTMENT OF DEFENSE

Assist to the Sec of Def, Atomic Energy
ATTN: Exec Assist

Defense Advanced Rsch Proj Agency
ATTN: Def Sciences Ofc

Defense Communications Agency
ATTN: Code J300
ATTN: WSE
ATTN: 900, D. Israel

Defense Intell Agency
ATTN: DB-4C2
ATTN: RTS-2A, Tech Lib
ATTN: RTS-2B

Defense Nuclear Agency
ATTN: RAEV
ATTN: SPSS
ATTN: STNA
ATTN: STSP
4 cys ATTN: STTI-CA

Defense Tech Info Ctr
12 cys ATTN: DD

Field Command, DNA, Det 2
Lawrence Livermore National Lab
ATTN: FC-1

DNA PACOM Liaison Office
ATTN: J. Bartlett

Field Command, Defense Nuclear Agency
ATTN: FCPR
ATTN: FCTO
ATTN: FCTT
ATTN: FCTT, W. Summa
ATTN: FCTXE

Field Command Test Directorate
ATTN: FCTBE, L. Ashbaugh

Joint Chiefs of Staff
ATTN: GD10, J-5, Nuc & Chem Dir

Joint Strat Tgt Planning Staff
ATTN: JLK, DNA Rep
ATTN: JLKC
ATTN: JPPFM
ATTN: JPPFN
ATTN: JPST
ATTN: JPTM

Under Secy of Def for Rsch & Engrg
2 cys ATTN: Strat & Space Sys (OS)

DEPARTMENT OF THE ARMY

BMD Advanced Technology Ctr
ATTN: ATC-T

BMD Systems Command
ATTN: BMDSC-HW
ATTN: BMDSC-LEE, R. Webb

DEPARTMENT OF THE ARMY (Continued)

Harry Diamond Laboratories
ATTN: DELHD-NW-P

US Army Ballistic Research Lab
ATTN: AMXBR-TBD, W. Taylor
ATTN: DRDAR-BLA-S, Tech Lib
ATTN: DRDAR-BLT, J. Keefer

US Army Concepts Analysis Agency
ATTN: CSSA-ADL, Tech Lib

US Army Corps of Engineers
ATTN: DAEN-ECE-T
ATTN: DAEN-RDL

US Army Engineer Ctr & Ft Belvoir
ATTN: DT-LRC

US Army Engineer Dist Omaha
ATTN: MROED-D, C. Distefano

US Army Engineer Div, Huntsville
ATTN: HNDED-SR
3 cys ATTN: C. Huang

US Army Engineer Div, Ohio River
ATTN: ORDAS-L, Tech Lib

US Army Engr Waterways Exper Station
ATTN: D. Banks
ATTN: Doc Con Off for Doc, J. Day
ATTN: H. Wilson
ATTN: J. Warringer
ATTN: Library
ATTN: P. Mlakar
ATTN: WESSD, J. Jackson
ATTN: WESSE
ATTN: WESSS, J. Ballard

US Army Information Systems Cmd
ATTN: B. Kappas
ATTN: Tech Ref Div

US Army Material Command
ATTN: DRXAM-TL, Tech Lib

US Army Nuc & Chem Agency
ATTN: Library

DEPARTMENT OF THE NAVY

Chief of Naval Opns, Dir Cmd Cont Plng & Prgmg Div
ATTN: OP-943

Naval Postgraduate School
ATTN: Code 1424, Library

Naval Research Laboratory
ATTN: Code 2627, Tech Lib

Naval Surface Weapons Ctr
ATTN: Tech Lib & Info Svcs Br

Naval War College
ATTN: Code E-11, Tech Svc

DEPARTMENT OF THE NAVY (Continued)

Ofc of the Dep Ch of Naval Ops
ATTN: NOP 981

Space & Naval Warfare Systems Cmd
ATTN: PDE-110-X1, B. Kruger

Strategic Systems Programs, PM-1
ATTN: NSP-43, Tech Lib

Submarine Force, US Pacific Fleet
ATTN: A. Stough

DEPARTMENT OF THE AIR FORCE

Air Force Institute of Technology
ATTN: Library

Air Force Ofc of Scientific Rsch
ATTN: J. Allen
ATTN: L. Hendrickson
ATTN: W. Best

Air Force Systems Command
ATTN: DLWM
ATTN: XRT

Air Force Weapons Laboratory
ATTN: D. Cole
ATTN: NTE, M. Plamondon
ATTN: R. Galloway
ATTN: SUL

Air University Library
ATTN: AUL-LSE

Assist Ch of Staff, Intelligence
ATTN: IN

Assist Ch of Staff, Studies & Analysis
ATTN: AFCSA/SAMI

Ballistic Missile Ofc/DAA
ATTN: CC-1
ATTN: CC-3
ATTN: EN
ATTN: ENS, W. Weisinger
ATTN: ENSN
ATTN: MGEN, E. Furbee
ATTN: SYB, L. Pothier
ATTN: SYBU, LT Michael
3 cys ATTN: ASMS

Dep Ch of Staff, Rsch, Dev & Acq
ATTN: AF/RDQI
ATTN: AFRD
ATTN: AFRD-M, A. Ravgiala

Foreign Technology Div
ATTN: NIIS, Library

Strategic Air Command
ATTN: DEPM
ATTN: DOM
ATTN: INAO
ATTN: NRI/STINFO
ATTN: XOKM
ATTN: XPFC
ATTN: XPFS
ATTN: XPQ

DEPARTMENT OF THE AIR FORCE (Continued)

Secretary of the Air Force
ATTN: SAFAL, S. Gold

DEPARTMENT OF ENERGY

Dept of Energy, Ofc of Mil Application, GTN
ATTN: OMA, DP-22

University of California
Lawrence Livermore National Lab
ATTN: G. Smith
ATTN: H. Heard
ATTN: L-47, D. Oakley
ATTN: Tech Info Dept Lib

Los Alamos National Laboratory
ATTN: C. Watson
ATTN: D 446, B. Killian
ATTN: J. Neudecker
ATTN: L. Germaine
ATTN: MS P364, Reports Library
ATTN: O. Hart
ATTN: T. Dey

Oak Ridge National Laboratory
ATTN: Central Rsch Lib

Sandia National Laboratories
ATTN: Lib & Security Class Div

Sandia National Laboratories
ATTN: Org 7111, L. Hill
ATTN: Tech Lib, 3141

OTHER GOVERNMENT AGENCIES

Central Intelligence Agency
ATTN: OSWR/NED

Dept of the Interior, Bureau of Mines
ATTN: Tech Lib

Dept of the Interior, US Geological Survey
ATTN: D. Roddy

Ofc of Technology Assessment
ATTN: R. Staffin

US Geological Survey
ATTN: R. Carroll
ATTN: W. Twenhofel

DEPARTMENT OF DEFENSE CONTRACTORS

Aerospace Corp
ATTN: Library Acquisition M1/199

Agbabian Associates
ATTN: C. Bagge
ATTN: D. VanDillen
2 cys ATTN: M. Agbabian

Analytic Services, Inc, ANSER
ATTN: K. Baker

Applied Research Associates, Inc
ATTN: N. Higgins
2 cys ATTN: S. Hassiotis

DEPARTMENT OF DEFENSE CONTRACTORS (Continued)

Applied Research Associates, Inc
ATTN: S. Blouin

Applied Research Associates, Inc
ATTN: D. Piepenburg

Applied Research Associates, Inc
ATTN: R. Frank

Applied Theory, Inc
ATTN: J. Trulio

AVCO Systems Div
ATTN: Library A830

BDM Corp
ATTN: Corp Lib
ATTN: T. Neighbors

BDM Corp
ATTN: E. Bultmann
ATTN: F. Leech
ATTN: M. Garcia

Bell Aerospace Textron
ATTN: C. Berninger
ATTN: R. Gellatly

Boeing Co
ATTN: Aerospace Lib
ATTN: H. Leistner
ATTN: M/S 42/37, K. Friddell
ATTN: T. Berg
2 cys ATTN: J. Wooster

California Institute of Technology
ATTN: D. Anderson

California Research & Technology, Inc
ATTN: K. Kreyenhagen
ATTN: Library
ATTN: S. Schuster

California Research & Technology, Inc
ATTN: F. Sauer

California Research & Technology, Inc
ATTN: Tech Lib

Calspan Corp
ATTN: Z. Zudans

Calspan Corp
ATTN: Library

Carpenter Research Corp
ATTN: H. Carpenter

University of Denver
ATTN: Sec Ofcr for J. Wisotski

EG&G Wash Analytical Svcs Ctr, Inc
ATTN: Library

Electro-Mech Systems, Inc
ATTN: R. Shunk

Foster-Miller Inc
ATTN: J. Hampson for E. Foster

DEPARTMENT OF DEFENSE CONTRACTORS (Continued)

GTE Communications Products Corp
ATTN: E. Courier
ATTN: R. Sullivan

H & H Consultants, Inc
ATTN: E. Cording
ATTN: J. Haltiwanger
ATTN: J. Hendron
ATTN: S. Paul

IIT Research Institute
ATTN: Doc Lib
ATTN: M. Johnson
ATTN: R. Welch

Institute for Defense Analyses
ATTN: Classified Lib

Kaman Sciences Corp
ATTN: Library

Kaman Sciences Corp
ATTN: Lib
ATTN: R. Keefe

Kaman Sciences Corp
ATTN: E. Conrad

Kaman Tempo
ATTN: DASIAC

Kaman Tempo
ATTN: DASIAC

Lockheed Missiles & Space Co, Inc
ATTN: J. Bonin
ATTN: Tech Info Ctr

Martin Marietta Denver Aerospace
ATTN: J. Gliozzi
ATTN: R. Haymen

Massachusetts Inst of Technology
ATTN: W. Brace

Merritt CASES, Inc
ATTN: D. Burgess
ATTN: J. Merritt

MITRE Corp
ATTN: Tech Report Ctr

University of New Mexico
ATTN: N. Baum

University of New Mexico
ATTN: M. Ostrower

City College of New York
ATTN: C. Miller

Northwestern University
ATTN: T. Belytschko

Pacific-Sierra Research Corp
ATTN: A. Laupa
ATTN: D. Wilson
ATTN: H. Brode, Chairman SAGE

DEPARTMENT OF DEFENSE CONTRACTORS (Continued)

Pacific-Sierra Research Corp
ATTN: D. Gormley

Pacifica Technology
ATTN: G. Kent

Patel Enterprises, Inc
ATTN: M. Patel

Physics International Co
ATTN: E. Moore

R&D Associates
ATTN: C. Lee
ATTN: C. Knowles
ATTN: D. Oberste-Lehn
ATTN: D. Simons
ATTN: J. Lewis
ATTN: P. Haas
ATTN: R. Mesic
ATTN: Tech Info Ctr

Rand Corp
ATTN: P. Davis

Rand Corp
ATTN: B. Bennett

S-CUBED
ATTN: C. Archembeam
ATTN: D. Grine
ATTN: K. Pyatt
ATTN: Library
ATTN: R. Duff

Science Applications Intl Corp
ATTN: H. Pratt
ATTN: M. McKay
ATTN: Technical Lib

Science Applications Intl Corp
ATTN: W. Layson

Science Applications, Inc
ATTN: Tech Lib

Southwest Rsch Institute
ATTN: A. Wenzel
ATTN: W. Baker

DEPARTMENT OF DEFENSE CONTRACTORS (Continued)

SRI International
ATTN: B. Holmes
ATTN: G. Abrahamson
ATTN: J. Bruce

Structural Mechanics Associates, Inc
ATTN: R. Kennedy

Terra Tek, Inc
ATTN: Library
ATTN: S. Green

Texas A & M University System
ATTN: J. Handin
ATTN: Sec Ofc for A. Rychlik

TRW Electronics & Defense Sector
ATTN: B. Balachandra
ATTN: N. Lipner
ATTN: P. Huff
ATTN: R. McFarland
ATTN: Tech Info Ctr

TRW Electronics & Defense Sector
ATTN: B. Keltner
ATTN: D. Randell
ATTN: E. Wong
ATTN: L. Woodruff
ATTN: O. Lev
ATTN: P. Dai
ATTN: R. StClair
ATTN: S. Rindskopf

Universal Analytics, Inc
ATTN: E. Field

Weidlinger Assoc, Consulting Engrg
ATTN: T. Deevy

Weidlinger Assoc, Consulting Engrg
ATTN: I. Sandler
ATTN: M. Baron

Weidlinger Assoc, Consulting Engrg
ATTN: J. Isenberg

William Perret
ATTN: W. Perret

R&D Associates
ATTN: G. Ganong

END

FILMED

5-86

DTIC